Estimation of Land-Based Pollution Loads to the Yellow Sea from the Han River

Final Report

January 2019

KOEM 해양환경공단

HydroCore
Experts in diffuse pollution modeling

SUMMARY

1 INTRODUCTION

1. Background

The Yellow Sea is a marginal sea of the Pacific Ocean covering a total of 458,000 km² surrounded by PR China and the Korean peninsula. Major rivers flowing to the Yellow Sea include the Yangtze River, the Huai River and the Yalu River (Aprok River) in PR China, the Aprok River (Yalu River) and the Daedong River in DPR Korea, the Han River and the Geum River in RO Korea. About 600 million people, which accounts for about 10% of the world's population, live along the rivers and the coast of the Yellow Sea (UNDP/GEF 2007). Moreover, a number of coastal zones of the Yellow Sea have been reclaimed and used as agricultural land, salt fields or aquafarms for fish, shrimps and shellfish. The dense population, intensive fisheries and large-scale agricultural and industrial activities have had serious environmental impacts on the Yellow Sea, impairing its ecosystem services. In particular, the increasing land-based pollution loads, mainly due to rapid urbanization and intensive agriculture, are very much concerned by both Korean and Chinese governments in recent years.

To effectively decrease the pollution loads to the Yellow Sea, it is critical to understand the spatio-temporal distributions of pollution loads. In RO Korea, there are four major river systems that flow to the Yellow Sea: The Han River, the Geum River, the Mankyoung-Dongjin River, and the Youngsan River. The pollution loads from each of these river systems need to be evaluated using a best available science-based methodology. To begin with, this study aims: (1) to set up a watershed model for the Han River Watershed; (2) to estimate the spatio-temporal distributions of pollution loads from the Han River Watershed to the Yellow Sea.

2 LITERATURE REVIEW

1. Status Quo of the Yellow Sea

The Yellow sea is a semi-enclosed shallow sea covering an area of around 458,000 km² with an average depth of only 46 m. Several major rivers from RO Korea (Han River, Geum River and Mankyoung-Dongjin River), DPR Korea (Aprok River and Daedong River) and PR China (Yangtze River, Huai River and Yalu River) flow to the Yellow Sea. It is connected to the Bohai Bay to the north and the East China Sea to the south. As for its biological diversity, there is a total of 1,964

species identified in the marine and coastal habitats of RO Korea alone. These species include 276 fishes, 199 water birds, 18 marine mammals, 500 marine invertebrates, 70 phytoplanktons, 300 benthic diatoms, 50 halophytes and 6 ascidians. In the Chinese region 1,140 species were recorded. In its coastal areas or along the rivers flowing to the sea, there are major cities including Tsingtao, Tianjin, Dalian, Shanghai, Seoul, Incheon, Pyongyang and Nampo, where about 600 million people live, which is approximately 10% of the world population.

Continuous increase of pollution loads have resulted in the increase of eutrophication. The frequency, extent, and duration of harmful algal blooms (HAB) have increased since the early 1970s. This has mainly been due to increased pollution loads of industrial, agricultural and aquacultural wastes. In 2002, a total of 79 HAB incidents were reported in the Chinese marine territory. The total area affected was over 10,000 km^2; among these incidences, 51 HAB cases were found in the East ChinaSea with the affected area exceeding 9,000 km^2, 17 HAB cases were found in the Yellow Sea and the Bohai Bay with the affected area of nearly 600 km^2.

2. Pollutions in Other Coastal Areas

The increasing land-based pollution loads, mainly due to rapid urbanization and intensive agriculture in the coastal areas, cause various environmental problems in coastal and marine habitats such as wetlands, mangrove forests and coral reefs. These problems include exploitation of marine resources, eutrophication, marine litter, anoxia, increasing nutrient discharge from agricultural land, and the inflow of heavy metals and other persistent pollutants from industrial plants. Major incidents include the deterioration of the Great Barrier Reef (GBR) ecosystem, hypoxia and algal blooms at the Bay of Bengal and excessive nutrient loadings into the Baltic Sea.

To effectively improve the environment of the Yellow Sea, cooperation between organizations are essential at both national and international level. Currently, various joint projects, action plans and international agreements are being implemented, including the United Nations Convention on the Law of the Sea (UNCLOS) to solve marine environmental problems, AGENDA 21 as an action plan for global conservation to realize sustainable development.

3. Estimation of Pollution Loads using Watershed Models

Watershed models are widely used to evaluate pollution loads from both point sources and diffuse sources. As most environmental issues of coastal areas are closely associated with the characteristics of the watersheds draining to the coastal areas, certain features of watershed models

such as mass balance analysis and scenario analysis are very useful to improve our scientific understandings of certain coastal processes and to derive reasonable alternatives.

Currently a wide range of various watershed models are being used to improve our understandings of the hydrologic and the hydrochemical processes within watersheds and to evaluate pollution loads from watersheds, at the regional or global scale. Such watershed models include: IMAGE-GNM (Integrated Model to Assess the Global Environment-Global Nutrient Model), Global News-2 (Nutrient Export from WaterSheds version 2), SPARROW (SPAtially Referenced Regressions on Watersheds), RVERSTRAHLER, SWAT (Soil and Water Assessment Tool), STREAM (Spatio-Temporal River-basin Ecohydrology Analysis Model) and AGNPS (AGricultural Non-Point Source pollution).

4. Coastal Management Policies

In recent years, RO Korea has witnessed negative changes in many marine ecosystems have been highlighted by media as one of the serious socio-economic issues. The Korean government has endavored to implement and enforce integrated coastal management by taking legal measures (the Coast Management Act, the Marine Environment Management Act, and the Conservation And Management Of Marine Ecosystems Act), science and technology development, and intensive investment in eco-friendly use of marine resources. In addition, the government policies have focused on improving the institutional systems and on establishing the infrastructure for conservation of the marine environment and ecosystem. Heavily polluted coastal areas are designated as the Coastal Areas Under Special Management (the coast of Busan and Ulsan, the Masan Bay, the Gwangyang Bay, and the Lake Sihwa). To control land-based diffuse pollution, the Ministry of Environment implemented environmental policies such as the Total Maximum Daily Load Management Programs (TMDLMP) and the Designated Diffuse Source Management Areas. The Ministry of Oceans and Fisheries also operates the TMDLMP for the Coastal Areas Under Special Management. Currently, the TMDLMP has been implemented and is in operation for the Masan Bay (2008), the Lake Sihwa (2013) and the coast of Busan (2015).

As global obligations to protect the marine environment are strengthened, discharges of various pollutants are strictly regulated, and discussions are increasingly active about international regulations to tighten the environmental criteria for the marine ecosystem. The 1992 UN Rio Declaration on Environment and Development was signed for sustainable growth of the global environment. Recommendations from Agenda 21 urge countries to develop and implement integrated coastal management (ICM) plans. In 1993, Land-Ocean Interactions in the Coastal Zone (LOICZ) was established as a core project for the International Geosphere-Biosphere Programme (IGBP) of the

International Council for Science (ICSU) to estimate and understand coastal environmental changes and trends.

In the United States, efforts to protect the marine environment are being made by enacting acts and developing systems for land-based pollution source management, habitat protection and restoration such as the Coastal Zone Management Act and the Federal Water Pollution Control Act. The Total Maximum Daily Load Management Programs of the U.S. is to improve water quality by developing and implementing plans for acceptable Total Maximum Daily Loads (TMDLs), under the circumstances that the target water quality cannot be met through traditional treatment techniques for water quality management specified in section 303(d) of the Clean Water Act.

Since 1979, Japan has been operating its Total Maximum Daily Load Management Programs for COD, nitrogen and phosphorus to improve the water quality of the enclosed waters. In accordance with this system, viable goals and target years are set and assigned to local governments and pollution sources.

3 ESTIMATION OF POLLUTION LOADS FROM THE HAN RIVER WATERSHED

1. Study Area

The Han River Watershed covers an area of 34,401.9 km^2 that accounts for 34.3% of the total area of RO Korea. As a part of the river networks run across the RO Korea-DPR Korea border, the watershed lies in between the two countries: about four-fifth of the watershed area (27,919.8 km^2, 81.2%) lies in RO Korea, and the rest one-fifth of the watershed area (6,482.1 km^2, 18.8%) lies in DPR Korea.

2. Methodology

The REDPOLL was set up for the Han River Watershed using grid cells of 100 m by 100 m and daily time steps for the year 2016. The rainfall and the temperature data observed at 18 monitoring stations in and around the Han River Watershed were collected and compiled for the model. The observed flow rates and water qualities of the discharges from main sewage treatment plants, the water abstractions from major dams within the watershed were collected and fed into the model. For estimating discharges from major dams, regression equations using the past observations of inflows, stages, and upstream rainfalls were derived and incorporated into the model. Spatial distributions of

topographic characteristics, land cover and soil texture were analyzed using the national data sets and compiled for the model.

The watershed model was calibrated against the flow rates and the water quality observed at the outlets of the 48 sub-watersheds. The evaluated PBIAS (Percent BIAS, %) values of the calibrated model for flow rate, SS, BOD, TN and TP are 28.5%, 66.8%, 30.5%, 21.0%, and 53.2%, respectively. Given that the monitoring data are discontinuous, observed only on every 8 days, the calibration results are considered to be fairly reasonable. It is particularly encouraging that the model calibration results of flow rates show very satisfactory (PBIAS = 16.0%, R^2 = 0.68) for 5 sub-watersheds where flow rates were observed continuously.

3. Results and Discussion

Flows and pollution loads to the Yellow Sea from the Han River Watershed were evaluated for the year 2016 based on the simulation results of REDPOLL. A water balance analysis of the Han River Watershed for the year 2016 show that out of the total annual precipitation of 1,100.6 mm/year (100%), evapotranspiration comprises 456.4 mm/year (41.5%), direct runoff and baseflow from the watershed comprise 629.2 mm/year (57.2%), and outflow to the Yellow Sea comprises 608.7 mm/year (56.2%).

For the year 2016, the annual total river flow from the Han River Watershed to the Yellow Sea is 21,286 x 10^6 m^3/year and the pollution loads are SS 836.5 x 10^3 ton/year, BOD 56.1 x 10^3 ton/year, TN 82.5 x 10^3 ton/year and TP 3.8 x 10^3 ton/year. River flows and pollution loads have a very wide range of daily and monthly variation. As affected by the monsoon weather system, the monthly volume of river flows in July reaches 7,484 x 10^6 m^3/month accounting for 35.2% of the annual discharge. Likewise, the monthly pollution loads in July comprise more than a quarter of the annual loads: SS 49.4%, BOD 40.0%, TN 30.9% and TP 41.6%.

In the Han River Watershed, the majority of pollution loads come from the diffuse source: SS 99.8%, BOD 86.8%, TN 75.2%, and TP 92.7%.

4 CONCLUSIONS AND SUGGESTIONS

1. Conclusions

The REDPOLL was set up for the Han River Watershed using grid cells of 100 m by 100 m and daily time steps for the year 2016. The watershed model was calibrated against the flow rates and the water quality observed at the outlets of the 48 sub-watersheds.

Flows and pollution loads to the Yellow Sea from the Han River Watershed were evaluated for the year 2016 based on the simulation results of REDPOLL. For the year 2016, the annual total river flow from the Han River Watershed to the Yellow Sea is 21,286 x 10^6 m^3/year and the pollution loads are SS 836.5 x 10^3 ton/year, BOD 56.1 x 10^3 ton/year, TN 82.5 x 10^3 ton/year and TP 3.8 x 10^3 ton/year. As affected by the monsoon weather system, the monthly volume of river flows in July reaches 7,484 x 10^6 m^3/month accounting for 35.2% of the annual discharge. Likewise, the monthly pollution loads in July comprise more than a quarter of the annual loads: SS 49.4%, BOD 40.0%, TN 30.9% and TP 41.6%.

In the Han River Watershed, the majority of pollution loads come from the diffuse source: SS 99.8%, BOD 86.8%, TN 75.2%, and TP 92.7%.

2. Policy Suggestions

In the context of the YSLME project, it is critical to estimate land-based pollution loads to the Yellow Sea from major river watersheds in RO Korea, DPR Korea, and PR China. For better understandings and development of effective national and international policies, it is of utmost importance to develop a common research framework for data sharing and common modeling platform among the three countries.

To effectively manage the land-based pollution loads to the Yellow Sea, it is necessary to extend the geographical range of this study to other major river watersheds in RO Korea, DPR Korea, and CPR China. For PR China, although the Bohai Bay is connected to the Yellow Sea, it is excluded from the scope of the YSLME project. Considering the potential biophysicochemical processes between the Bohai Bay and the Yellow Sea, the Bohai Bay and its watersheds should be included in the YSLME project. As for DPR Korea, despite some of the DPR Korean rivers flow to the Yellow Sea, DPR Korea is not participating in the YSLME project for some reason. Both RO Korean and Chinese authorities need to invite DPR Korean authority and should put more effort into establishing the partnership with DPR Korea in the context of this project.

To successfully restore and manage the ecosystem, it is important to identify, evaluate and implement effective measures for land-based pollution sources. The Ministry of Environment is responsible for the land environment while the Ministry of Oceans and Fisheries is in charge of the marine environment. Although the land and the sea are connected to each other in nature, they are

separately managed by the two ministries. It is therefore critical to establish a tight coordination system, such as liaison officers, between the two ministries to manage land-based pollution sources more efficiently and effectively.

Table of Contents

Figures

Tables

1 INTRODUCTION

1.1 Background

The Yellow Sea is a marginal sea of the Pacific Ocean covering an area of around 458,000 km² surrounded by PR China and the Korean peninsula (Figure 1). In geographical terms, the sea is located at 117-126 degrees of longitude and 31-41 degrees of latitude. Its average depth is 46 m with its deepest point less than 80 m (WWF and KIOST, 2014).

The Yellow Sea is connected to some major Chinese rivers such as the Yangtze River. It also receives discharges from the rivers in DPR Korea (the Aprok River and Daedong River) and RO Korea (the Han River, the Geum River and the Mankyoung-Dongjin River). The sediments transported from these rivers form an intertidal zone with a total area of about 20,000 km² in the sea (Barter, 2002). It is reported that every year the Yellow Sea receives 46 million tons of precipitation, 1.6 billion tons of sediments and 1,500 billion tons of water from rivers (UNDP/GEF, 2013).

Figure 1. The Yellow Sea surrounded by PR China and the Korean peninsula

According to the Moores *et al*. (2001), there are a total of 1,964 species identified in the marine and coastal habitats of RO Korea alone. These species include 276 fishes, 199 water birds, 18 marine mammals, 500 marine invertebrates, 70 phytoplanktons, 300 benthic diatoms, 50 halophytes and 6 ascidians. In the Chinese region 1,140 species were recorded (Moores *et al*., 2001). The Yellow Sea is not only a very productive sea, but also an important part of the world fishery routes.

Major rivers draining to the Yellow Sea include the Yangtze River, the Huai River, and the Yalu River (Aprok River) in PR China, the Aprok River (Yalu River) and the Daedong River in DPR Korea, the Han River and the Geum River in RO Korea. Approximately 600 million people, which accounts for about 10% of the world's population, live along the rivers and the coast of the Yellow Sea (UNDP/GEF 2007). Moreover, a number of coastal zones of the Yellow Sea have been reclaimed as agricultural land, salt fields or aquafarms for fish, shrimps and shellfish. The agricultural land in the coastal areas of the sea has been expanded to 63 million hectares in total, which reportedly makes up about 60% of the entire area of the Chinese farms. The dense population, intensive fisheries and large-scale agricultural and industrial activities have had serious environmental impacts on the Yellow Sea, impairing its ecosystem services. In particular, the increasing land-based pollution loads, mainly due to rapid urbanization and intensive agriculture, are very much concerned by both Korean and Chinese governments in recent years.

The frequency of red tides has increased in the Yellow Sea since the mid-1980s due to the increase of pollution loads from land. In recent years, the number and extent of red tides in the sea have been growing due to industrialization, population density and rising water temperature. Bashkin *et al*. (2002) evaluated the nitrogen accumulation in the Yellow Sea by estimating the inputs (e.g. atmospheric deposition, fertilizer application, biological fixation, and imported foods and feed) and the outputs (e.g. stream discharge, crop uptake, denitrification, volatilization and runoff), based on the data collected between 1994 and 1997. They concluded that the nitrogen accumulation in the Yellow Sea was 1,229 kt/year, and the nitrogen residence time was about 1.5 years. According to the study, the nitrogen accumulation doubled during the study period (1994 - 1997).

In 2008, macroalgae *Enteromorpha prolifera* bloomed in the Yellow Sea, where approximately 100 million dollars were spent to remove and control the algae. Gilbert (2013) examined the changes of macroalgae in the Yellow Sea for 10 years using satellite photos and found out that *E. prolifera* covered less than 21 km^2 in 2007 but the coverage rapidly increased to 1,900 km^2 in 2008, and 1,600 km^2 in 2009. Such a dramatic increase was due to high nutrient loads, including sewage discharges, and aquaculture of seaweeds (*Porphyra yezoensis*, nori) between 2007 and 2008. When a large quantity of *E. prolifera* decompose, they produce ammonia and hydrogen sulfide that can be harmful for human and marine organisms.

Land-based pollution, in particular, can have serious adverse effects on the marine ecosystem and could ultimately lead to the depletion of fishery resources. To effectively decrease the pollution loads to the Yellow Sea, it is critical to understand the spatio-temporal distributions of pollution loads from the watersheds that drain to the Yellow Sea. In RO Korea, there are four major river systems that flow to the Yellow Sea: the Han River, the Geum River, the Mankyoung-Dongjin River, and the Youngsan River. The pollution loads from each of these river systems need to be evaluated. To begin with, this study aims: (1) to set up a watershed model for the Han River Watershed; (2) to estimate the spatio-temporal distributions of pollution loads from the Han River Watershed to the Yellow Sea.

1.2 Objectives and Scope of the Study

1.2.1 Objectives

The objectives of this study are as follows:

- To set up a watershed model for the Han River Watershed
- To estimate the spatio-temporal distributions of pollution loads from the Han River Watershed to the Yellow Sea

1.2.2 Scope of the study

1) The Han River Watershed

The main study area is the Han River Watershed that drains to the Yellow Sea (Figure 2). The total area of the Han River Watershed is 34,401.9 km^2 that accounts for 34.3% of the RO Korean territory. As a part of the river networks run across the RO Korea-DPR Korea border, the watershed lies in between the two countries: about four-fifths of the watershed area (27,919.8 km^2, 81.2%) lies in RO Korea, and the rest one-fifth of the watershed area (6,482.1 km^2, 18.8%) lies in DPR Korea.

2) Individual tasks

The scope of this study is set as follows:

- To review previous studies on the Yellow Sea, potential pollution sources, watershed modeling, and public policies
- To estimate pollution loads from the Han River Watershed using a watershed model
- To suggest policy related implications

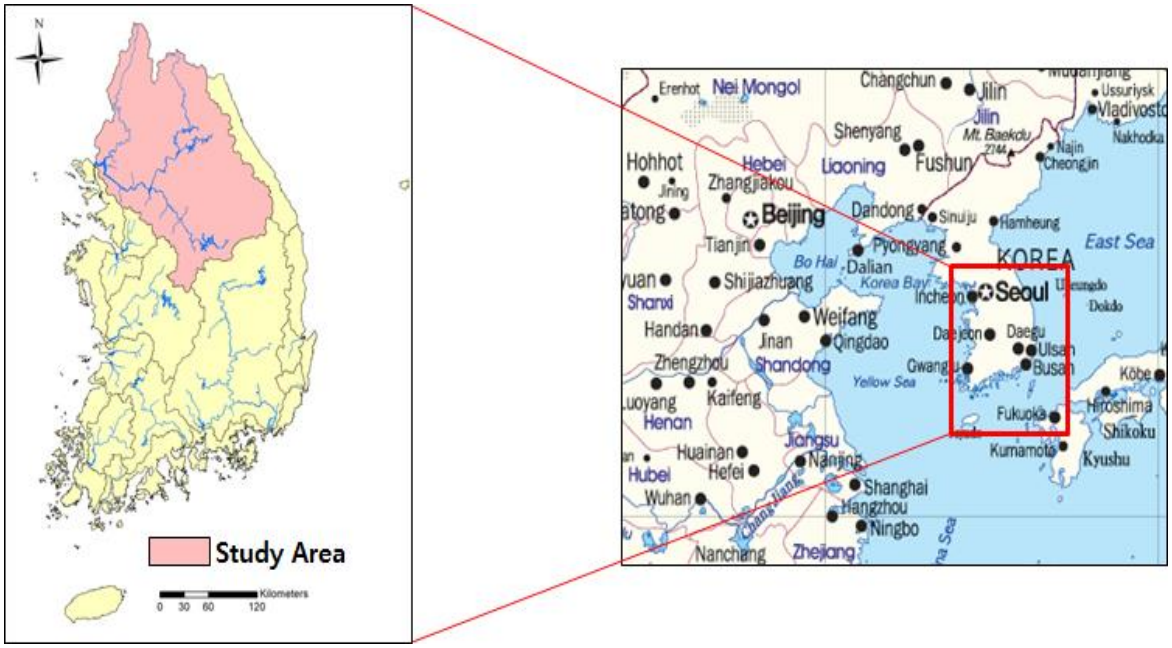

Figure 2. Location of the study area: The Han River Watershed

2 LITERATURE REVIEW

2.1 Status Quo of the Yellow Sea

2.1.1 Introduction

The Yellow sea is a semi-enclosed shallow sea covering an area of around 458,000 km² with an average depth of only 46 m. Several major rivers from RO Korea (Han River, Geum River and Mankyoung-Dongjin River), DPR Korea (Aprok River and Daedong River) and PR China (Yangtze River, Huai River and Yalu River) flow to the Yellow Sea. It is connected to the Bohai Bay to the north and the East China Sea to the south.

The Yellow Sea receives a large amount of sediment each year (1.6 billion tons per year) mainly from the Yellow river and the Yangtze river (Teng *et al*., 2005). The surface water temperature of the Yellow Sea may go below the freezing point during winter and form ice covers. During summer, however, the water temperature may rise to as high as 27 - 28°C (Teng *et al*., 2005).

Lying between PR China and the Korean peninsula major cities including Qingdao, Tianjin, Dalian, Shanghai, Seoul/Incheon, and Pyongyang-Nampo are located near the coasts or rivers that drain to the Yellow Sea (Figure 3). This accounts for approximately 600 million inhabitants, which is almost 10% of the world's population (WWF and KIOST, 2014).

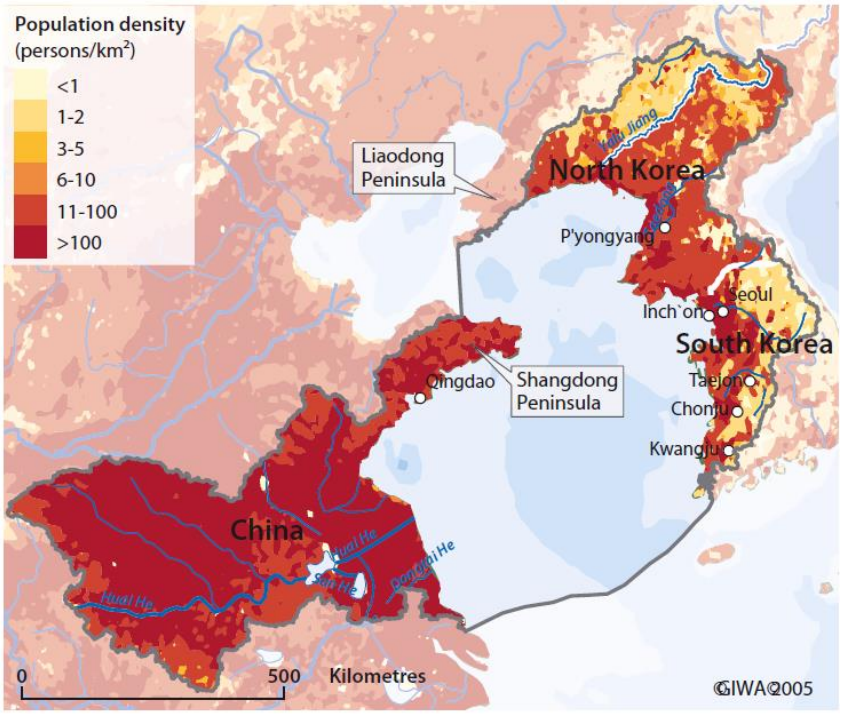

Figure 3. Population density in the Yellow Sea region (Teng *et al*., 2005)

The Yellow Sea is one of the most intensively exploited areas in the world. The number of commercially harvested species counts to about 100 species, including cephalopods and crustaceans. The abundance of most species is relatively low, and only 23 species exceed 10,000 tons in annual catch. Demersal species used to be the major part of the catch and accounted for 65 to 90% of the annual total catch. The resource populations of demersal species such as Small Yellow Croaker (*Pseudosciaena polyctis*), Hairtail (*Trichiurus haumela*), Large Yellow Croaker (*Pseudosciarna crocea*), Flatfish (*Pleuronectis* sp.), and Cod (*Gadus* sp.) declined in biomass by more than 40% when fishing efforts increased three folds from the early 1960s to the early 1980s (Teng *et al*., 2005).

2.1.2 Water quality and biodiversity

Among the world's 64 Large Marine Ecosystems (LMEs), the Yellow Sea LME has been one of the most significantly affected by human development. Continuous increase of pollution loads has resulted in the increase of eutrophication. The frequency, extent, and duration of harmful algal blooms (HAB) have increased since the early 1970s. This has been mainly due to increased pollution loads of industrial, agricultural and aquacultural wastes. Natural disasters such as typhoons that bring up excessive amounts of bottom nutrients are also a contributor (She, 1999). In addition, HAB organisms may be transported by shipping traffic, as well as from the huge discharge from the Yangtze River (Changjiang) during the summer monsoon season, which sometimes reaches the southern end of the Korean peninsula (MOE 2003). In 2002, a total of 79 HAB incidents were reported in the Chinese marine territory. The total area affected was over 10,000 km^2; among these incidences, 51 HAB cases were found in the East China Sea with the affected area exceeding 9,000 km^2, 17 HAB cases were found in the Yellow Sea and the Bohai Bay with affected area of nearly 600 km^2 (SEPA, 2004). Eutrophication in freshwater rivers and lakes in the region also occurs frequently, causing depletion of dissolved oxygen content (less than 2.0 mg/l) in the water leading to fish kills and changes in plankton species composition in coastal waters (SEPA, 2004).

According to the Moores *et al*. (2001), there is a total of 1,964 species identified in the marine and coastal habitats of RO Korea alone. These species include 276 fishes, 199 water birds, 18 marine mammals, 500 marine invertebrates, 70 phytoplankton, 300 benthic diatoms, 50 halophytes and 6 ascidians. In the Chinese region 1,140 species were recorded (Moores *et al*., 2001). Marine animals such as spotted seals, herrings, pacific cods, blue mussels, abalones, sea snakes and other species of the temperate zone feed and breed in the Yellow Sea. However, environmental problems, such as overexploitation, pollution loads and habitat destructions due to land reclamations, are threatening the biodiversity of the Yellow Sea. Even the species of high biodiversity have suffered and will suffer high levels of loss. It has been estimated that around 80 species of birds are classified as threatened in the regions of PR China and RO Korea (Baker, 2002).

2.2 Pollutions in Other Coastal Areas

2.2.1 Environmental impact of land-based pollutions on coastal areas

With rapid urbanization and economic development along the coast, the impacts of land-based anthropogenic activities on coastal and offshore marine habitats, such as coastal wetlands, mangroves and coral reefs, have significantly increased. Major problems include degradation of marine biodiversity due to overexploitation of marine resources, coastal eutrophication, ocean acidification, costal and marine litter, increased nutrient loads (nitrogen and phosphorus) from agricultural farms and heavy metals and organic pollutants from industries.

The Great Barrier Reef (GBR), which is the world's largest coral reef, is located along the north-east coast of Australia extending over 2000 km (Kroon *et al*., 2016). The GBR ecosystem consists of variety of tropical marine habitats, such as coral reefs, seagrass meadows and mangrove forests. Due to the recognition of natural significance, high levels of national and international protection were established. However, the GBR ecosystem has continuously deteriorated over time mainly due to land-based pollution which has been exacerbated by impacts of climate change. It has been estimated that the coral cover declined by 50% for the whole GBR and by 70% along the developed central and southern GBR from 1985 to 2012(De'ath *et al*., 2012). The population of many species, including sharks, stingrays, sea snakes, marine turtles, seabirds, dolphins and dugongs, have significantly decline especially in central and southern inshore areas (Great Barrier Reef Marine Park Authority, 2014). River loads of suspended sediments, nitrogen, phosphorus and pesticides have increased by 2 - 9 times since the 1850s.

The Baltic Sea is well-renowned for its heavy loads of nitrogen and phosphorus input. The annual total nitrogen input is estimated to approximately one million tons and phosphorus input approximately 50,000 tons. The main sources of nutrients are from adjacent watersheds of agriculture, municipalities and industries. Nutrient emissions from agricultural areas share a big part amongst all sources. Since the 1950's the increased usage of fertilizers is correlated with the increase of average phosphate and nitrate concentrations (Kremser and Schnug, 2002). Excessive nutrient emission causes eutrophication, increased planktons biomass and oxygen deficiencies. It has been identified that there are about 30 harmful phytoplankton species distributed in the Baltic Sea. In 1998, the bloom of *Chrysochromulina polylepis* has caused trouble to fish farms and killed marine organisms (Kremser and Schnug, 2002).

The Bay of Bengal is located on the northeastern part of the Indian Ocean. Approximately 200 million people live along the Bay of Bengal's coasts and of these a major proportion are partially or wholly dependent on its fisheries (BOBLME, 2015). Ten Major rivers, such as the Ganges, Irrawaddy, Cauweri, Danidarm, Penner, Brahmaputra, Meghna, Mahanadi, Godavari, Krishna and Salween River

s flow to the Bay with large volumes of freshwater and silt, especially during the monsoon season (from July to September). In 2000, rivers exported 7.1 Tg-N and 1.5 Tg-P to the Bay of Bengal (Pedde *et al*., 2017). Three rivers (Ganes, Godavari, Irrawaddy) account for 75-80% of the total river export of Nitrogen and Phosphorus. Pedde *et al*. (2017) estimated an increase in river export of dissolved N (by 40%) and P (by 80%) due to losses from agriculture and sewage systems. Hypoxia and algal blooms have been observed along the coastlines of the BOBLME. Hypoxia may be harmful to the aquatic ecosystems and result in dead zones, and harmful algal blooms may cause socio-economic problems threatening fisheries and tourism (Bricker *et al*., 2008).

2.2.2 Management of land-based pollutions in coastal areas

Marine ecosystem management is not only an issue of a single country but also involves cooperation and interactions from many countries around the globe. For this reason, there have been numerous collaborative projects, action plans and international treaties to resolve environmental problems of the marine ecosystem.

In 1982, the United Nations established an international treaty, United Nations Convention on the Law of the Sea (UNCLOS), to define rights and responsibilities of nations to respect their use of the world's oceans and provide guidelines to manage the environment and marine natural resources (Hoagland *et al*., 2001). It came into force in 1994. In 2016, 167 countries and the European Union have joined the treaty (Guo, 2018). In the treaty, article 207 specifically states the management of pollution from land-based sources. Hence, countries have to adopt laws and regulations to prevent, reduce and control pollution of the marine environment from land-based sources, including rivers, estuaries, pipelines and outfall structures, taking into account internationally agreed rules, standards and recommended practices and procedures (UN, 1994).

The Agenda 21 is a program of action for sustainable development worldwide (UNDESA, 2012). It was adopted in 1992 at the Earth Summit (UN Conference on Environment and Development) held in Rio de Janeiro, Brazil. It consists of 40 chapters that identify challenges and propose simple realistic solutions towards sustainable development. Chapter 17 of the Agenda deals with the "Protection of the oceans, all kinds of seas, including enclosed and semi-enclosed seas, and coastal areas and the protection, rational use and development of their living resources". It aims to set out appropriate action, objectives, activities and implementation to protect and preserve the marine environment and pursue sustainable usage of marine resources and sustainable development. Moreover, chapter 17.24 – 17.29 specify the actions needed to be taken to prevent, reduce and control marine environment from land-based sources of pollution (Hassan, 2017).

The countries of BOBLME region, Sri-Lanka, India, Bangladesh, Myanmar, Thailand, Indonesia, Malaysia and Maldives, agreed to work together to manage their shared living resources through the preparation of a regional Strategic Management. This concerned threats of health and productivity of the BOBLME due to pollution from land-based sources. Consequently, their main priorities lied on management of land-based sources of pollution from sewage, agriculture/aquaculture and industries.

2.3 Estimation of Pollution Loads using Watershed Models

2.3.1 Introduction

Land-based pollution sources can be classified into two groups: point sources and diffuse sources. The definitions of point sources and diffuse sources are as follows, respectively:

- Point Sources: Any discernable, confined and discrete conveyance, including but not limited to any pipe, ditch, channel, tunnel, conduit, well, discrete fissure, container, rolling stock, concentrated animal feeding operation, or vessel or other floating craft, from which pollutants are or may be discharged. This term does not include agricultural storm water discharge and return flows from irrigated agriculture (Section 502 (14) of the Clean Water Act).
- Diffuse Sources: Any source of water pollution that does not meet the legal definition of "point source" in section 502(14) of the Clean Water Act. Or diffuse pollution caused by runoff due to rainfall or snowmelt moving over and through the ground. The water absorbs and assimilates any pollutants it comes into contact with and is discharged into lakes, rivers, wetlands, coastal waters and ground waters (USEPA, 2004).

Watershed models are widely used to evaluate pollution loads from both point sources and diffuse sources. As many coastal environmental problems are closely associated with the characteristics of the watersheds that drain to the coastal areas, certain features of watershed models such as mass balance analysis and scenario analysis are very useful to improve our scientific understandings of certain coastal processes and to derive reasonable alternatives.

Currently a wide range of watershed models are being used to improve our understandings of the hydrologic and the hydrochemical processes within watersheds and to evaluate pollution loads discharged from watersheds, at the regional or global scale. Such watershed models include: IMAGE-GNM (Integrated Model to Assess the Global Environment-Global Nutrient Model), Global News-2 (Nutrient Export from WaterSheds version 2), SPARROW (SPAtially Referenced Regressions on Watersheds), RVERSTRAHLER, SWAT (Soil and Water Assessment Tool), STREAM (Spatio-

Temporal River-basin Ecohydrology Analysis Model) and AGNPS (AGricultural Non-Point Source pollution).

Global NEWS-2 model estimates river export of nitrogen (N), phosphorus (P), carbon (C) and silica (Si) at the river estuary in different forms (dissolved inorganic, dissolved organic and particulate). This model was applied to the coastal waters of the Bohai Bay, Yellow Sea and South China Sea to analyze the export of nutrients through the rivers (Strokal *et al*., 2014).

MARINA (Model to Assess River Inputs of Nutrients to seAs) is a downscaled version for PR China of the Global NEWS-2 which quantifies river export of nutrients by source at the sub-watershed scale as a function of human activities (nutrient losses from animal production and population) for PR China. This model was applied to six large rivers draining to the Bohai Bay (Yellow River, Hai River, Liao River), the Yellow Sea (Yangtze River, Huai River) and the South China Sea (Pearl River) to quantify dissolved inorganic and organic nitrogen and phosphorus in 1970, 2000, and 2050 (Strokal *et al*., 2016).

A semi-distributed watershed model STREAM (Spatio-Temporal River-watershed Ecohydrology Analysis Model) has been applied to estimate pollution loads to estuaries and coastal waters in RO Korea including the Geum River Estuary, Lake Sihwa, Gangjin Bay and Tongyeong-Jaran Bay. The STREAM is highly applicable to agricultural areas where paddy fields are distributed across the watershed, as the model estimates water abstractions and surface runoffs considering the irrigation controls in accordance with the growth stages of rice (Jeong *et al*., 2018).

2.3.2 Classification of watershed models

A watershed model can be described as empirical, conceptual, or physical according to the type of basic equations that the model employs to represent hydrologic processes. Empirical models use non-linear relationship between inputs and outputs and conceptual models use simplified conceptual equations while physical models employ physically-based equations. A comparison of the basic structure for watershed models is summarized in Table 1 (USEPA, 2017).

The spatial structure of a watershed model can be described as lumped, semi-distributed or distributed based on input data requirements and how runoff is generated and routed over the watershed. Lumped models assume the watershed is homogeneous and ignore spatial variability of the watershed processes. Semi-distributed models employ a series of lumped and distributed parameters for sub-watersheds and distributed models normally use square grids to account for spatial variability of the watershed processes. A comparison of the spatial structures in watershed models is summarized in Table 2 (USEPA, 2017).

Table 1. Comparison of the basic structure for watershed models (USEPA, 2017)

	Empirical	Conceptual	Physical
Method	Non-linear relationship between inputs and outputs, black box concept	Simplified equations that represent water storage in catchment	Physical laws and equations based on real hydrologic responses
Strengths	Small number of parameters needed, can be more accurate, fast run time	Easy to calibrate, simple model structure	Incorporates spatial and temporal variability, very fine scale
Weaknesses	No connection between physical catchment, input data distortion	Does not consider spatial variability within catchment	Large number of parameters and calibration needed, site specific
Best Use	In ungauged watersheds, runoff is the only output needed	When computational time or data are limited.	Have great data availability on a small scale
Examples	Curve Number, Artificial Neural Networks	HSPF, TOPMODEL, HBV, Stanford	MIKE-SHE, KINEROS, VIC , PRMS

Table 2. Comparison of the spatial structures in watershed models (USEPA, 2017)

	Lumped	Semi-distributed	Distributed
Method	Spatial variability is disregarded; entire catchment is modeled as one unit	Series of lumped and distributed parameters	Spatial variability is accounted for
Inputs	All averaged data by catchment	Both averaged and specific data by sub-catchment	All specific data by cell
Strengths	Fast computational time, good at simulating average conditions	Represents important features in catchment	Physically related to hydrological processes
Weaknesses	A lot of assumptions, loss of spatial resolution, not ideal for large areas	Averages data into subcatchment areas, loss of spatial resolution	Data intense, long computational time
Examples	Empirical and conceptual models, machine learning	Conceptual and some physical models, TOPMODEL, SWAT	Physically distributed models, MIKESHE, VELMA

2.4 Coastal Management Policies

2.4.1 National policies of RO Korea

1) The Coastal Areas Under Special Management

The growing public concerns for the marine environment and the need for sustainable use of marine resources have urged the government to take necessary actions. Consequently, the Ministry of Oceans and Fisheries was established in 1996 and the national management system for the marine environment and ecosystem has effectively implemented. The implementation and reinforcement of the integrated coastal management have been taken forward by legalization of Acts (the Coast Management Act, the Marine Environment Management Act, and the Conservation and Management of Marine Ecosystems Act), development of science and technology, and investments on sustainable use of marine resources. Moreover, the MOF's policies have focused on improving the management systems and establishing infrastructure for the conservation of marine environment and ecosystem. In this context, five heavily polluted coastal areas are designated as the Coastal Areas Under Special Management (the coast of Busan, the Masan Bay, the Gwangyang Bay, the coast of Ulsan, and the Lake Sihwa) (Figure 4)

2) Total Maximum Daily Load Management Programs

In order to effectively improve the quality of fresh waters, the Ministry of Environment has introduced the Total Maximum Daily Load Management Programs (TMDLMPs) in 1999. A TMDLMP aims to achieve the target water quality (administrative goals) by improving the efficiency of water quality management and strengthening the responsibility for each of the economic entities within the TMDLMP region. For the watersheds of the Nakdong River, the Geum River, the Youngsan River and the Seomjin River, the second phase (2011-2015) has been completed and the third phase (2016-2020) is currently under implementation. For the Han River Watershed, the first phase (2013-2020) is under implementation.

The Ministry of Oceans and Fisheries is also operating TMDLMPs for the Coastal Areas Under Special Management to mitigate the land-based pollution loads to those areas. Currently the TMDLMPs are implemented for the Masan Bay (2008), Lake Sihwa (2013), the Busan coast (2015), and the Ulsan coast (2018) as shown in Table 3. These coastal areas cover only 1.26% (1,263 km^2) of the entire RO Korean territory, but the population comprises 16.1% of the national population and the population density is 4,568 people/ km^2 which is over 9 times higher than the national average.

Table 3. The Coastal Areas Under Special Management where TMDLMPs are implemented (Ministry of Oceans and Fisheries, 2015)

Coastal Areas Under Special Management	Phase of TMDLMP	Target Pollutants
Masan Bay	The second-phase TMDLMP (2012-2016)	COD, TP
Lake Sihwa	The first-phase TMDLMP (2013-2017)	COD, TP
Busan coast	The first-phase TMDLMP (2015-2019)	COD
Ulsan coast	The first-phase TMDLMP (2018-2022)	Copper, zinc and mercury
Gwangyang Bay	To be implemented in the near future	-

Figure 4. The five coastal areas designated for the Coastal Areas Under Special Management in RO Korea (Ministry of Oceans and Fisheries, 2015)

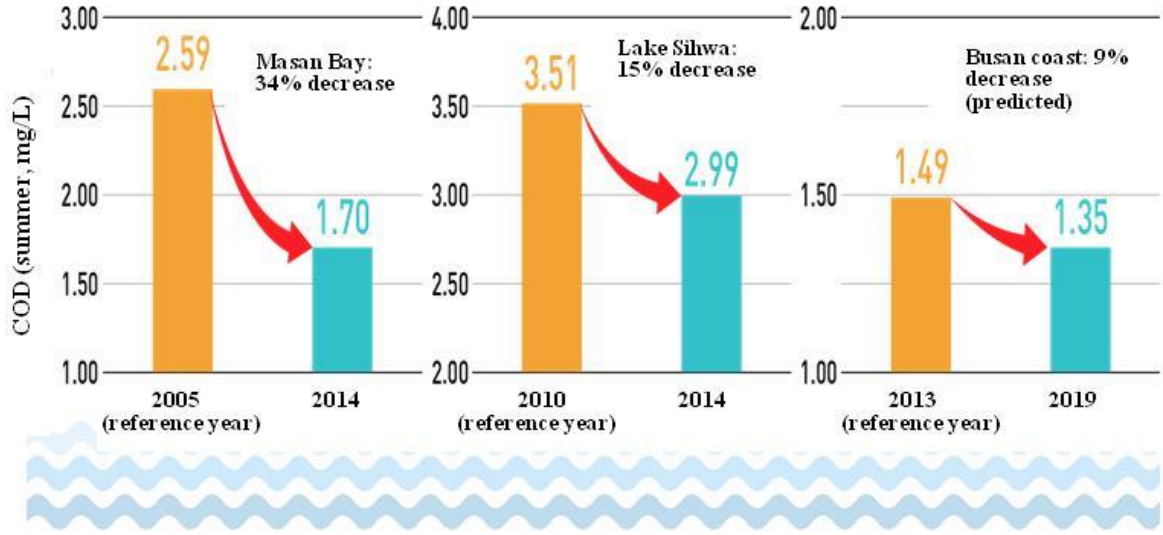

Figure 5. The decrease of COD concentrations after implementing TMDLMPs (Ministry of Oceans and Fisheries, 2015)

It has been reported that the water quality of the Coastal Areas Under Special Management significantly improved after the TMDLMPs have implemented. The average COD concentrations have decreased 34% in the Masan Bay, 15% in the Lake Sihwa, and 9% (prediction) in the coast of Busan (Figure 5).

2.4.2 International policies

1) International regulations on marine environment

As global obligations to protect the marine environment are strengthened, discharges of various pollutants are strictly regulated, and discussions are increasingly active about international regulations to tighten the environmental criteria for the marine ecosystem. The 1992 UN Rio Declaration on Environment and Development was signed for sustainable growth of the global environment. Recommendations from Agenda 21 urge countries to develop and implement Integrated Coastal Management (ICM) plans. In 2002, the workshop on the usage of assessment indicators in the ICM, organized by the Intergovernmental Oceanographic Commission (IOC), suggested procedures for developing, implementing and changing basic plans for coastal management areas. In June 2012, the 12 key assessment subjects selected at the RIO +20 conference include “the Extent of Achievement of Ecosystem-Based, Integrated Ocean and Coastal Management (Assessment 3)” and “Protection of the Marine Environment (Assessment 4)” (Table 4).

In 1993, Land-Ocean Interactions in the Coastal Zone (LOICZ) was established as a core project for the International Geosphere-Biosphere Programme (IGBP) of the International Council for Science (ICSU) to estimate and understand coastal environmental changes and trends. The study of bio-geo-chemical processes involved in the inflow and circulation of substances to coastal zones from land, rivers, groundwater and the atmosphere. The program aims to provide appropriate measures for the sustainable management of the coasts to policy makers and promote integrated coastal management, cooperation and joint research at local, national and global levels.

Table 4. Twelve key subjects of assessment of the Rio +20 in 2012

No	Subject

Assessment 1	The Status of Ocean Ecosystems and Coastal Communities, in the Context of Climate Change and Continuing Biodiversity Loss
Assessment 2	Addressing Critical Uncertainties for the Management of the Marine Environment and Climate Change
Assessment 3	The Extent of Achievement of Ecosystem-Based, Integrated Ocean and Coastal Management
Assessment 4	Protection of the Marine Environment
Assessment 5	The Status and Prospects for Fisheries and Aquaculture Within and Outside of National Jurisdiction
Assessment 6	The Special Issues Associated with Small-Island Developing States (SIDS) and Oceans, Especially in the Context of Climate Change
Assessment 7	Biodiversity Loss, Climate Change, and Networks of Marine Protected Areas
Assessment 8	Integrated Water Resources Management
Assessment 9	Financing
Assessment 10	Capacity Building, and Public Outreach
Assessment 11	The Role of the Oceans in the New Low-carbon Green Economy
Assessment 12	Improved International Environmental Governance

2) Land-based pollution management systems in the United States of America

The United States of America made efforts to protect the marine environment by implementing acts and developing the systems for land-based pollution source management, habitat protection and restoration such as the Coastal Zone Management Act and the Federal Water Pollution Control Act (Table 5). According to the Coastal Zone Management Act, the coastal management authority of each of the States should evaluate whether the Coastal Zones are properly designated for the management of land and water resources that can affect coastal water quality, and should adjust the Coastal Zones,

if necessary. The “Coastal Diffuse Pollution Management Program” (CDPMP) is operated by the National Oceanic and Atmospheric Administration (NOAA) and the U.S. Environmental Protection Agency (USEPA). For the implementation of the CDPMP, each of the coastal States should include relevant policies and tools.

Table 5. Summary of land-based pollution management and habitat protection in the U.S.

Acts	Relevant Authorities	Content
Coastal Zone Management Act	- Department of Commerce (National Oceanic and Atmospheric Administration) - Environmental Protection Agency - Department of Interior (US Fish and Wildlife Service) - State governments	- Coastal Management Program - Estuarine Research Reserve System - Coastal Resource Improvement Program - Coastal Zone Management Enhancement Program - Coastal Diffuse Pollution Management Program - Guidance for specifying management measures for sources of diffuse pollution in coastal waters
Federal Water Pollution Control Act	- Environmental Protection Agency - State governments	- Regulation on discharges of pollutants discharge into the waters of the United States of America - National Pollutant Discharge Elimination System (NPDES) - Diffuse source management program - National Estuary Program (NEP) - Regulation on discharges of dredge/fill material - Coastal recreation water quality monitoring

The Coastal Zone Management Act of the United States implies the importance of a close cooperation between the Ministry of Oceans and Fisheries and the Ministry of Environment of RO Korea to control land-based pollution sources more efficiently.

To improve and conserve the environment, the United States aims to select and apply effective and cost-efficient methods for integrated pollution management, total pollution load regulation, point source management with the National Pollutant Discharge Elimination System (NPDES) and

pollution source management with the best management practice (BMP). Since 1991, the USEPA is making efforts to meet the water quality standards by implementing the Total Maximum Daily Loads (TMDLs) for BOD, COD, TN, TP, heavy metals and other pollutants that occur in nature or from point or diffuse sources. Point-source pollution loads are regulated by the NPDES and pollution loads to navigable waters require NPDES permits.

The United States operates the Chesapeake Bay Program and the Puget Sound Partnership Program, which are among the most successful examples of the Integrated Coastal Management (ICM). The Chesapeake Bay is an estuarine bay on the eastern shore to the Atlantic Ocean. It covers a watershed area of about 165,760 km^2, consisting more than 150 rivers and tributaries and 17 million inhabitants (Figure 6a). The Chesapeake Bay has an average depth of only 6.4 meters, but its salinity varies widely depending on the locations. The Chesapeake Bay is home to diverse marine organisms and abundant with valuable marine resources. Since the early 20^{th} Century, a growing number of people began to inhabit near the coastal areas. Due to the increase of population many environmental problems have occurred on the bay, such as land use alteration, huge inflow of pollution as a result of environmental damage, anoxic layers created by stratification, toxic accumulation, and reduced marine resources. To solve these problems, the Chesapeake Bay Program was established based on an agreement signed by the governors of Maryland, Pennsylvania and Virginia, the mayor of Columbia, the EPA and the Chesapeake Bay Commission in 1983. The Chesapeake Bay Program is the first watershed management program in the United States operated under the principle of policies for environmental improvements conducted based on the participation and agreement of stakeholders (federal, state and local governments, community groups and the public) with a common goal to "Restore the Chesapeake Bay" (Figure 6b).

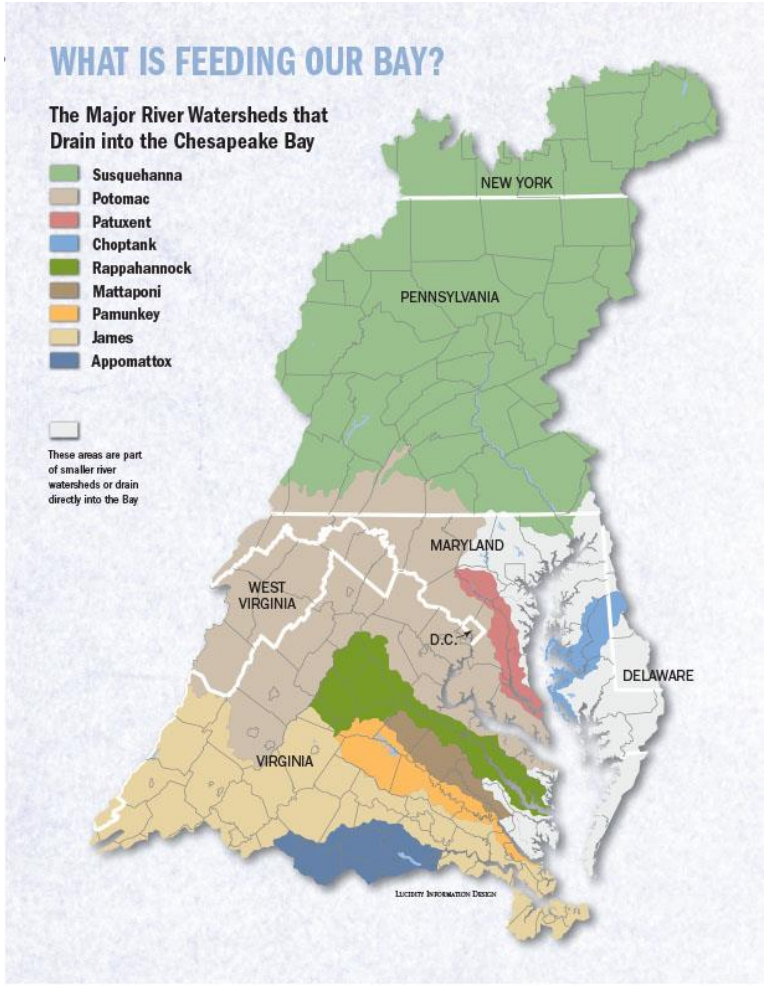

(a) The Chesapeake Bay Watershed

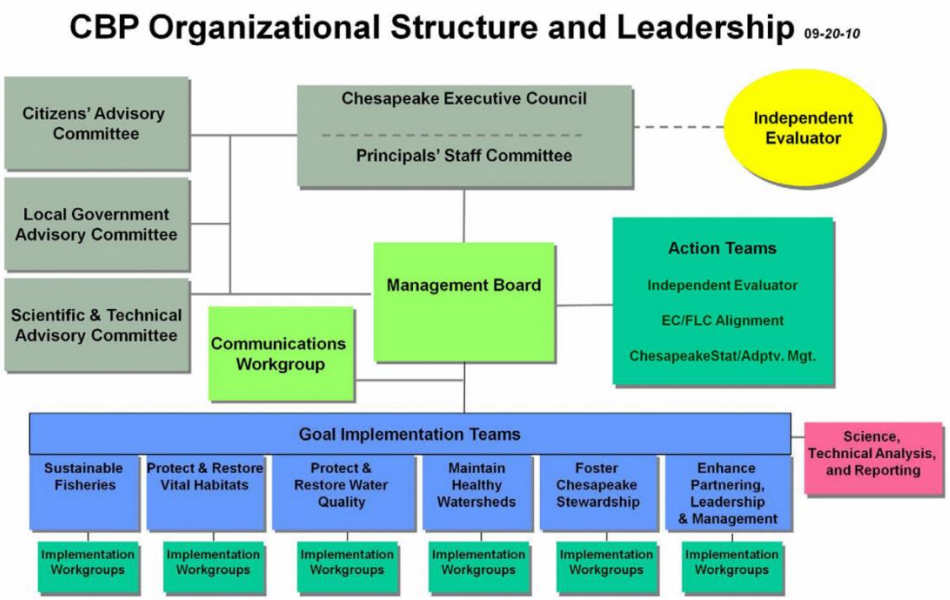

(b) Organizational structure of the Chesapeake Bay Program

Figure 6. The Chesapeake Bay Watershed and the organizational structure of the Chesapeake Bay Program (USEPA, 2010)

During the 1960s and 1970s, serious environmental damage of the Puget Sound resulted in the growth of public concerns. Consequently, the Washington State legislature founded the Puget Sound Water Quality Authority in 1985. In 2007, the Puget Sound Partnership (PSP) Program was established to restore the health of the Puget Sound. In 1987, the Puget Sound Water Quality Authority developed the Puget Sound Water Quality Management Plan and continued to update it to add new program elements. In 1987, the U.S. Congress defined the National Estuary Program (NEP) in section 320 of the Clean Water Act as a national issue. In 1991, the EPA recognized the Puget Sound Management Plan as a federal plan for comprehensive watershed conservation and management. The goals of the Puget Sound Management Plan are: (1) to preserve and restore the natural processes and functions of wetlands, aquatic habitats and their components; (2) to control the increasing pollution loads from watersheds; and (3) to reduce and eliminate risk factors of pollution loads to the seas, sediments and coasts; and to restore the biological health of the Puget Sound.

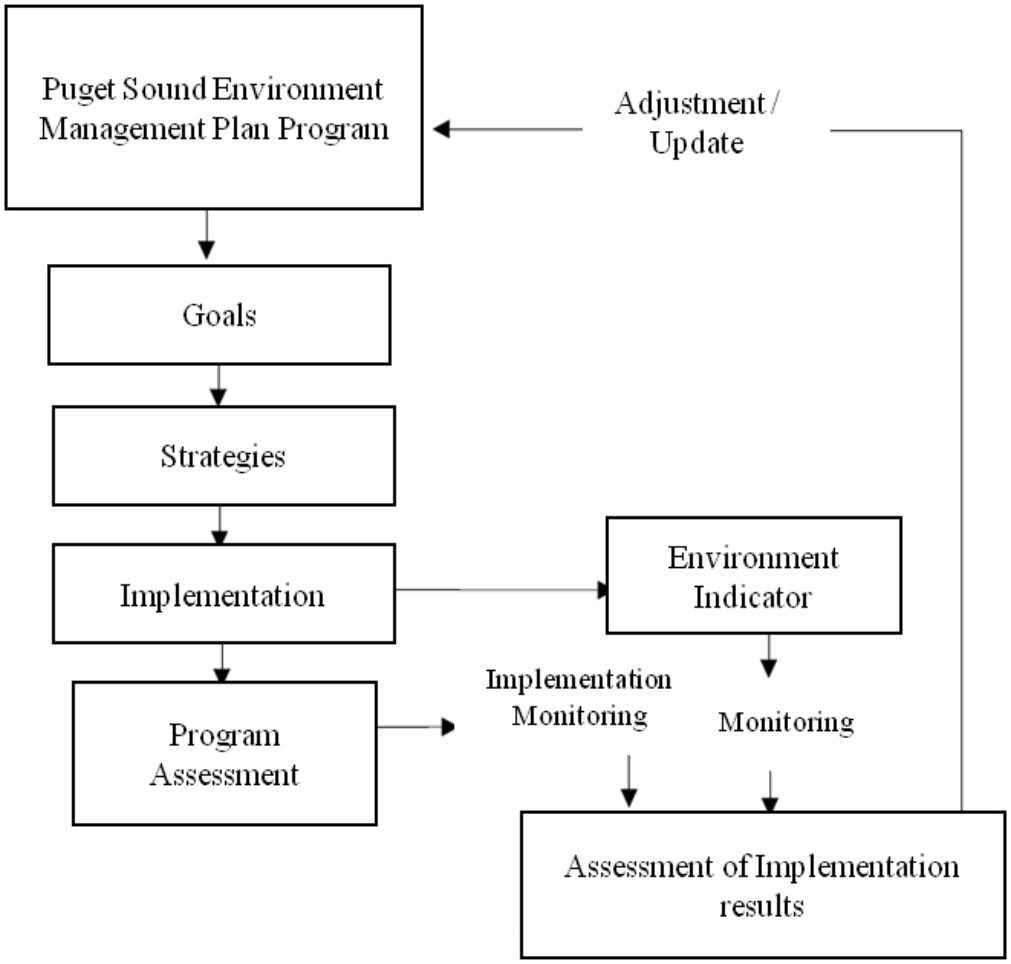

Figure 7. The flow chart of the Puget Sound Environment Management Plan enforcement process and feedback of the Puget Sound Management Plan

3) The Total Maximum Daily Load Programs in United States

The Total Maximum Daily Load (TMDL) Programs of the United States is to improve water quality by developing and implementing plans for acceptable TMDLs, under the circumstances that the target water quality cannot be met through traditional treatment techniques for water quality management specified in section 303(d) of the Clean Water Act. For U.S. estuaries and coastal waters, such as the Chesapeake Bay and Puget Sound, an integrated atmosphere-watershed-ocean modeling system has been established to provide water quality improvement measures and analyze policy alternatives for total pollution load management. The functions of this system have continually improved over the last three decades to support rational decision making. The U.S. TMDLs are enforced in all watersheds that exceed the regulated water quality standards. A total of 51 States and five U.S. territories (American Samoa, Guam, N. Mariana Islands, Puerto Rico and Virgin Islands) have developed and implemented TMDLs since October 1995. Furthermore, the EPA grouped these 51 States and five U.S. territories into 10 regions as illustrated in Figure 8, and provides TMDL reports, program summaries and guidance documents.

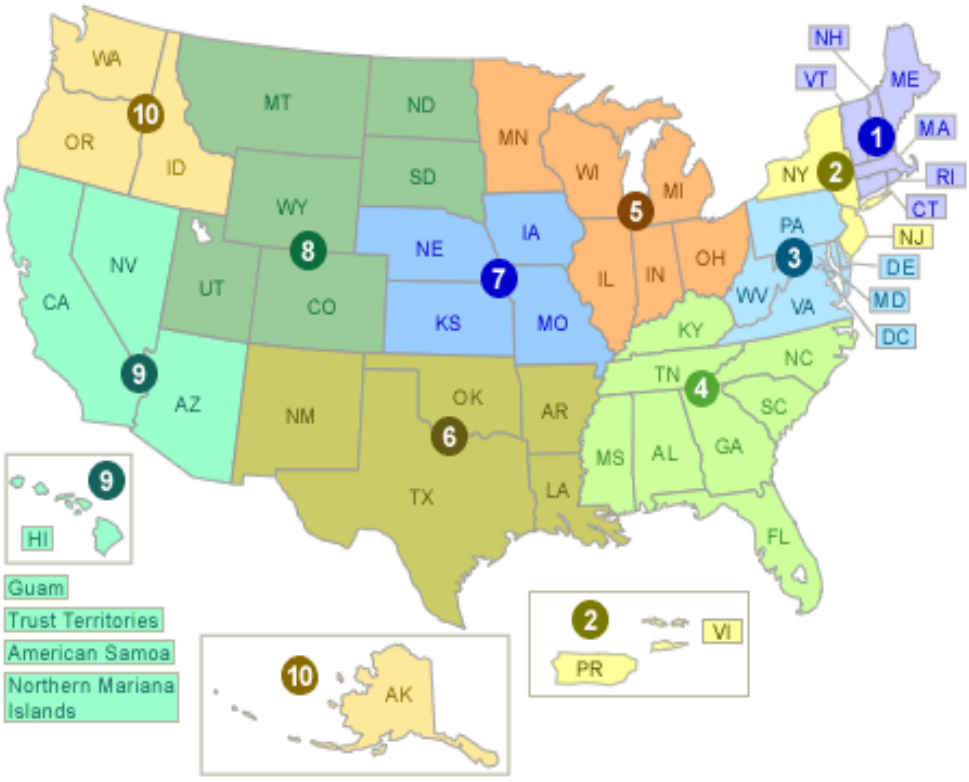

Figure 8. TMDL regions defined by the USEPA (USEPA homepage)

From October 1995 to 2016, a total of 69,205 TMDLs have been set to manage 72,653 impairments (Figure 9). TMDLs apply to all pollutants for which criteria have been provided. Since October 1995, mercury accounts for the largest portion (21,545) of the total TMDL cases followed by pathogens, metals, nutrients, sediments and water temperature. To conduct a TMDL, state governments first investigate and list waters that fail or could possibly fail to meet water quality goals, and submit the list to the EPA for approval. After receiving approval from the EPA, the state governments develop TMDLs for selected areas in the order of their management priority.

Fiscal Year	Number of TMDLs	Number of Causes of Impairment Addressed
1996	135	136
1997	337	351
1998	402	408
1999	330	373
2000	1,558	1,585
2001	2,581	2,617
2002	2,735	2,815
2003	3,008	3,281
2004	3,393	3,651
2005	4,319	4,634
2006	4,206	4,557
2007	4,321	4,651
2008	9,264	9,546
2009	4,399	4,623
2010	2,572	2,708
2011	2,830	3,113
2012	2,883	3,151
2013	15,534	15,624
2014	3,338	3,511
2015	945	1,068
2016	115	250

Figure 9. Annual number of TMDL approvals (from October to the following September) (USEPA homepage)

4) The Total Maximum Daily Load Programs in Japan

Since 1979, Japan has been operating its Total Maximum Daily Load Programs (TMDLP) for COD, nitrogen and phosphorus to improve water quality of semi-enclosed waters. In accordance with this program, viable goals and target years are set every 5 years and are assigned to the local governments and eventually to the individual pollution sources (Table 6). It requires the local governments and the pollution sources to reduce pollution loads, to set reduction targets based on the data of population and industrial growth, wastewater treatment technique levels and sewage treatment rates and to develop relevant policies (every five years). It is currently applied to the three semi-enclosed waters: Tokyo Bay; Ise Bay; and Seto Inland Sea (Figure 10).

Table 6. Timeline of the Total Maximum Daily Load Programs in Japan (Chungbuk Research Institute, 2009)

Enforcement	TMDL Programs	Period
Mar. 1980	The 1st TMDL program on COD	1979 - 1984
Apr. 1987	The 2nd TMDL program on COD	1984 - 1989
Mar. 1991	The 3rd TMDL program on COD	1989 - 1994
Sep. 1996	The 4th TMDL program on COD	1994 - 1999
Jul. 2002	The 5th TMDL program on COD, nitrogen and phosphorus	1999 - 2004
Jul. 2005	The 6th TMDL program on COD, nitrogen and phosphorus	2004 - 2009

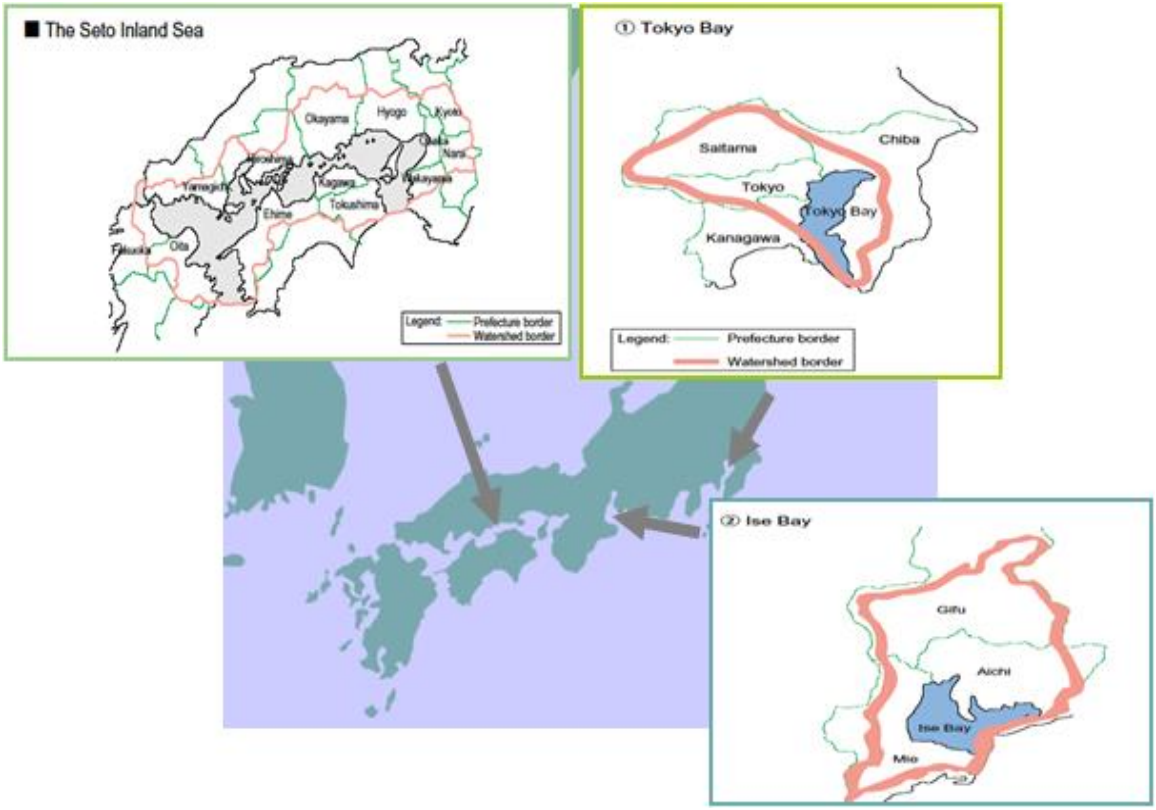

Figure 10. TMDL management areas in Japan (Ministry of the Environment, Japan)

3 ESTIMATION OF POLLUTION LOADS FROM THE HAN RIVER WATERSHED

3.1 Study Area

The Han River Watershed covers an area of 34,401.9 km^2 that accounts for 34.3% of the RO Korean territory (Figure 11). As a part of the river networks run across the RO Korea-DPR Korea border, the watershed lies in between the two countries: about four-fifths of the watershed area (27,919.8 km^2, 81.2%) lies in RO Korea, and the rest one-fifth of the watershed area (6,482.1 km^2, 18.8%) lies in DPR Korea.

The downstream area of the Han River Watershed is occupied by large cities such as Seoul and Incheon. The population in the Han River Watershed has steadily increased from less than 9 million in 1960s to over 20 million in recent years (Figure 12). Being densely populated, the watershed is highly vulnerable to pollution discharges from point sources, such as wastewater treatment plants, and diffuse sources, such as impervious surfaces at urban areas and crop lands. Moreover, the number of industrial operators in the agri-industrial complexes, in Seoul, Incheon and Gyeonggi-do, has increased (Figure 13) from 27,432 in 2007 to 46,864 in 2015. Industrial activities, among others, are more likely to discharge heavy pollution loads. The growing number of industrial operators can result in the increase of point source pollution loads.

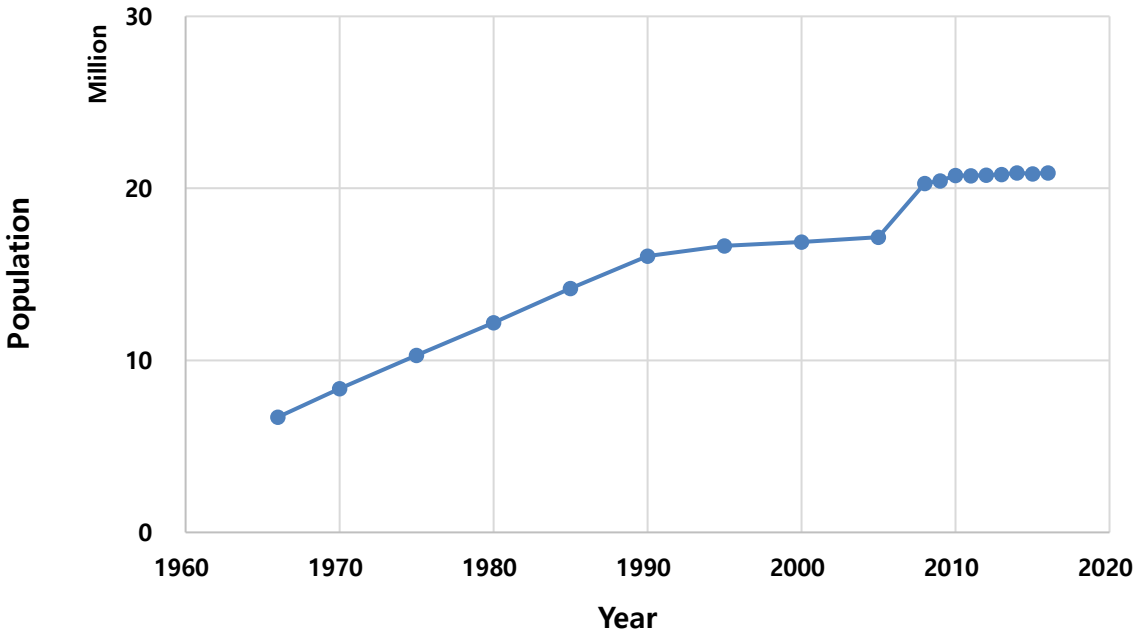

Figure 11. The changes of the total population in the Han River Watershed (www.wamis.go.kr)

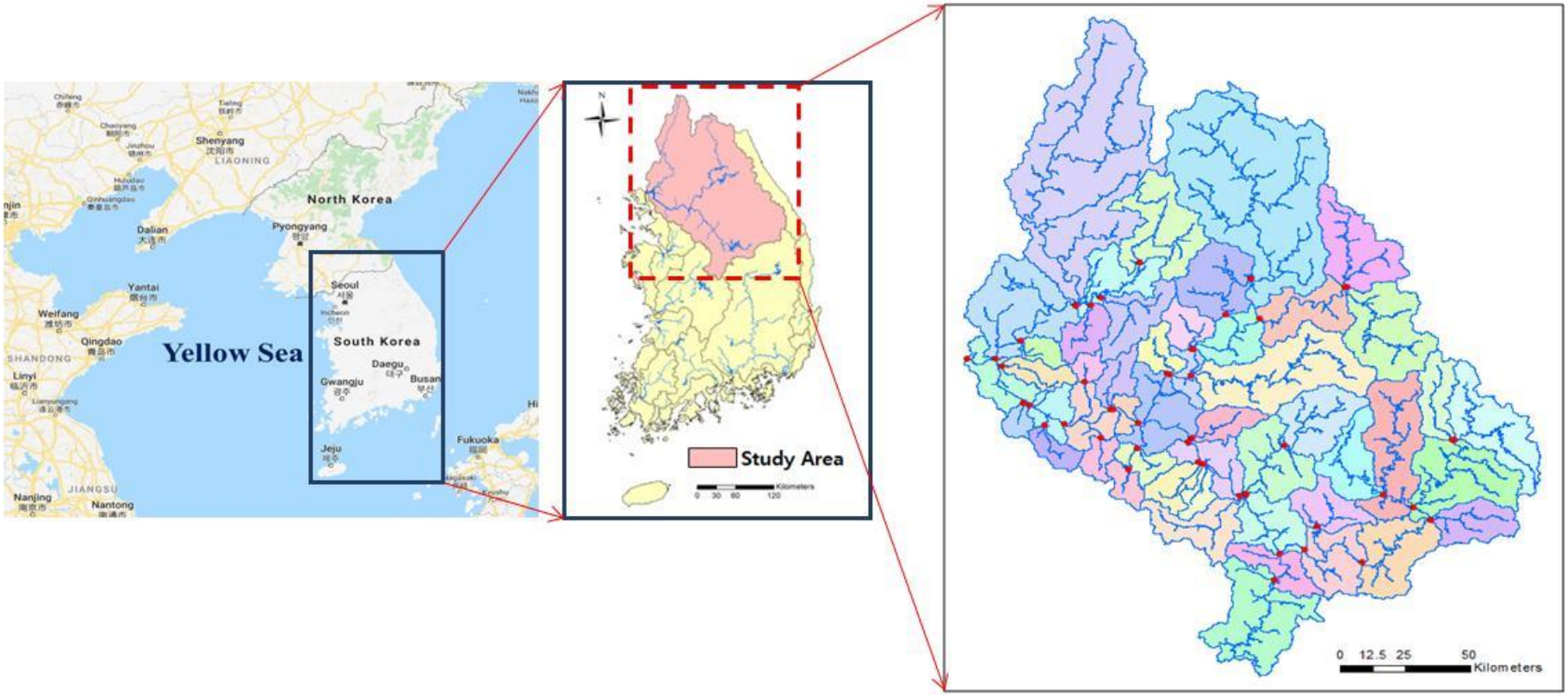

Figure 12. The location of the study area: The Han River Watershed

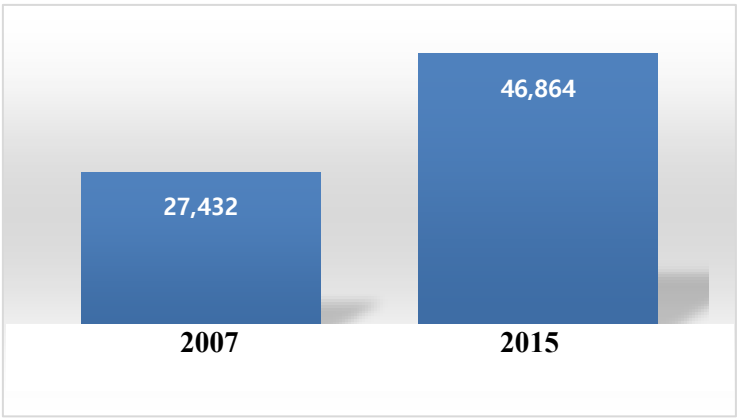

Figure 13. Number of industrial operators in Seoul, Incheon and Gyeonggi-do within the Han River Watershed in 2007 and 2015 (www.wamis.go.kr)

Land use changes in the Han River Watershed from 1975 to 2010 are presented in Table 7 and Figure 14 – Figure 16. The urban area increased about 4 times (323.2 km^2 in 1975 to 1,608.4 km^2 in 2010) and the diffuse pollution potential from impervious surfaces increased accordingly. The paddy fields decreased 62% from 5,173.3 km^2 in 1975 to 1,932.7 km^2 in 2010, while the dry fields increased about 10 times from 185.6 km^2 in 1975 to 1,847.5 km^2 in 2010. Despite the total area of paddy fields and dry fields decreased 29% from 5,358.9 km^2 in 1975 to 3,780.2 km^2 in 2010, the pollution loads from agricultural diffuse sources would have increased because the fertilizer application rates increased and the risk of soil erosion has greatly increased along with the increase of dry field area.

Table 7. The changes of land use area in the Han River Watershed (km^2) from 1975 to 2010

Year	Urban area	Paddy field	Dry field
1975	323.2	5,173.3	185.6
1980	498.7	5,000.6	403.6
1985	618.6	3,627.4	1,455.4
1990	771.6	3,607.6	1,620.1
1995	1,010.2	3,660.1	1,525.1
2000	1,128.4	3,669.5	1,671.8
2006	1,478.3	2,189.6	1,964.3
2010	1,608.4	1,932.7	1,847.5

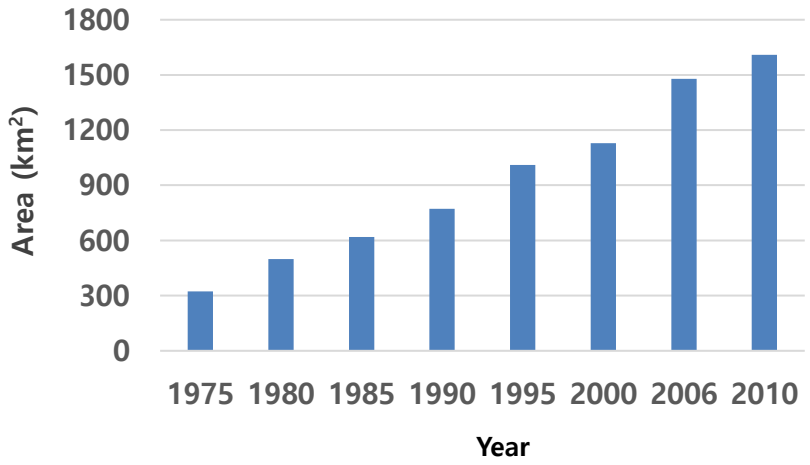

Figure 124. The total urban area in the Han River Watershed from 1975 to 2010

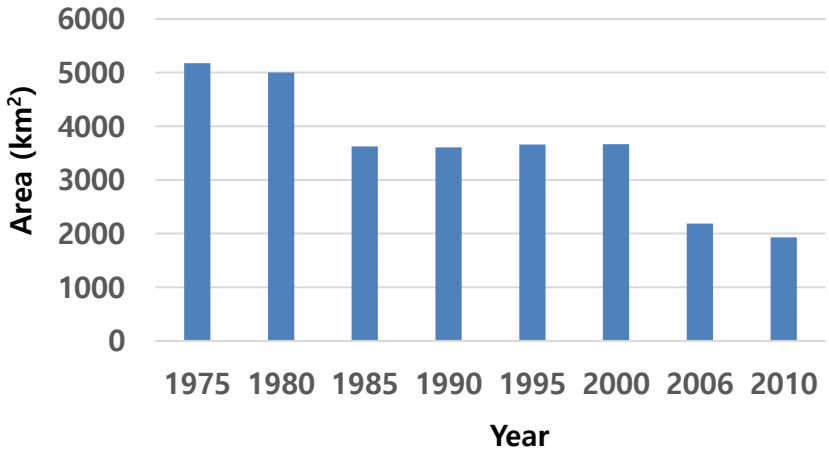

Figure 15. The total paddy field area in the Han River Watershed from 1975 to 2010

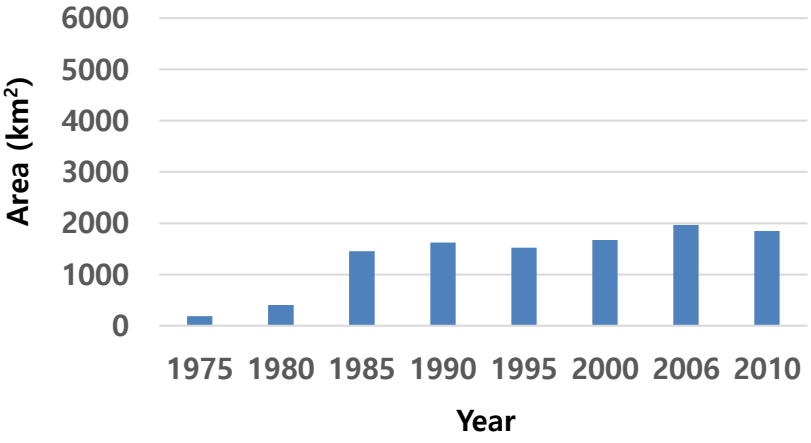

Figure 16. The total dry field area in the Han River Watershed from 1975 to 2010

3.2 Methodology

3.2.1 Model selection

Taking into account the study scope, the limitations in data availability and the future potential for extensions, the selection criteria for the watershed model for this study are set as the following:

- The model has appropriate structures to estimate pollution loads from both point and diffuse sources;
- The model is suitable to be applied to a large watershed for a long period of time;
- The model can represent spatio-temporal distributions of pollution loads;
- The model's data requirement is low;
- The model's source codes are accessible for future modifications.

Table 8 summarizes a comparison of five candidate watershed models against the selection criteria: L-THIA, REDPOLL, HSPF, SWAT and STREAM. Using the above criteria, REDPOLL (Regional Estimation of Diffuse POLlution Loads) was selected as the watershed model for this study. REDPOLL represents a watershed using a network of square grid cells. The model simulates hydrological processes using the SCS-CN methodology, and estimates pollution loads on a daily basis

Table 8. A comparison of five candidate watershed models against the selection criteria

Criteria	L-THIA	REDPOLL	HSPF	SWAT	STREAM
Watershed representation	Semi-distributed (HRUs)	Distributed (Square grids)	Semi-distributed (Sub-basins with HRUs)	Semi-distributed (Sub-basins with HRUs)	Distributed (Square grids)
Temporal scale	Daily	Daily	1 min. to 1 day	Daily	1 min. to 1 hour (variable time steps)
Hydrology	Conceptual (SCS CN method)	Conceptual (SCS CN method)	Conceptual	Conceptual (SCS CN method)	Physically-based and conceptual
Data requirement	Low	Low	High	High	High
Source code availability	No	Yes	Yes	Yes	Yes

using the event mean concentrations (EMCs) observed for different types of land uses. REDPOLL can represent spatio-temporal distributions of pollution loads from diffuse sources within a large watershed for a period of several years or more. As an intermediate-level model, REDPOLL does not require a heavy input data set and it can be set up and run with a relative ease. The source code of REDPOLL can be fully accessed by the Korean government for future extensions, if required.

3.2.2 The REDPOLL model

1) Overview

REDPOLL (Regional Estimation of Diffuse POLlution Loads) has been developed to evaluate the spatio-temporal pollution loads of large watersheds. It was applied in this study to estimate the daily flow rates and pollution loads from the Han River Watershed to the Yellow Sea. Figure 17 illustrates the process of applying the REDPOLL model to a watershed. Firstly, the watershed boundary is delineated to define the study area and the watershed is discretized by using topography and river network data. Then the temporal and spatial input data sets are prepared for the model set up. REDPOLL requires daily precipitation, daily temperature, topography, land use and soil texture. The model is calibrated and validated for certain periods of time against the observed flow and water quality data. The calibration process involves model accuracy assessment comparing the simulated data against the observed data. When the calibration is complete, the simulation period is set. The watershed processes are respectively simulated for hydrologic processes and transport of pollutants. Hydrologic processes include precipitation, evapotranspiration, direct runoff, groundwater discharge and river discharge. Attenuation of pollutants in the course of transport is simulated for suspended solids (SS), biochemical oxygen demand (BOD), total nitrogen (TN) and total phosphorus (TP).

REDPOLL discretizes a watershed into square grid cells, each of which consists of a soil layer and an aquifer layer. A watershed is composed of multiple sub-watersheds that are connected to one another by node-link networks using the upstream-downstream structure (Figure 18).

In REDPOLL, the hydrologic process is simulated using three types of storages: grid cells, sub-watershed and channel (stream). In a grid cell, hydrologic processes such as precipitation, infiltration, evapotranspiration, groundwater recharge, surface runoff and baseflow occur. The baseflow and surface runoff from grid cells are aggregated in the sub-watershed and stored in a virtual water storage. The discharge from the virtual water storage is routed to the watershed outlet through the river network of node-link structure taking into account the topographic characteristics of the watershed (Figure 19).

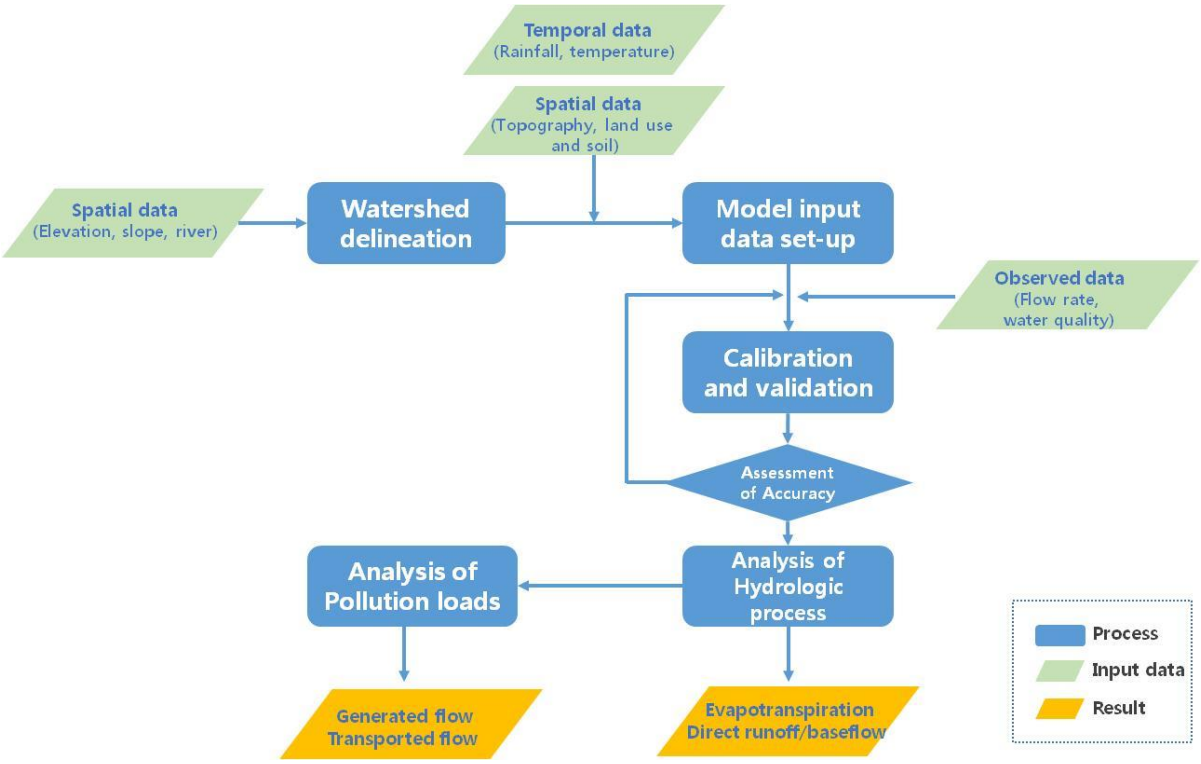

Figure 17. A diagram showing the process of applying REDPOLL to a watershed

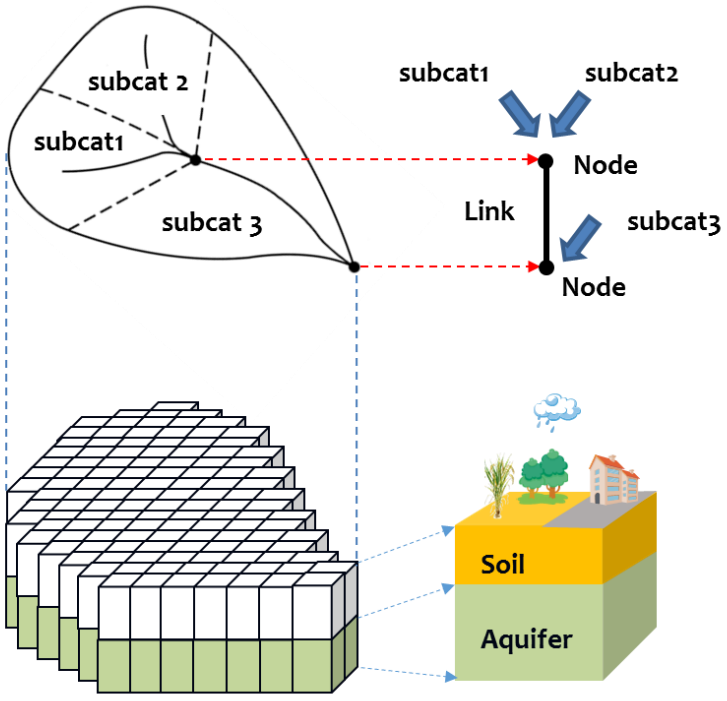

Figure 18. REDPOLL represents a watershed using a network of square grid cells

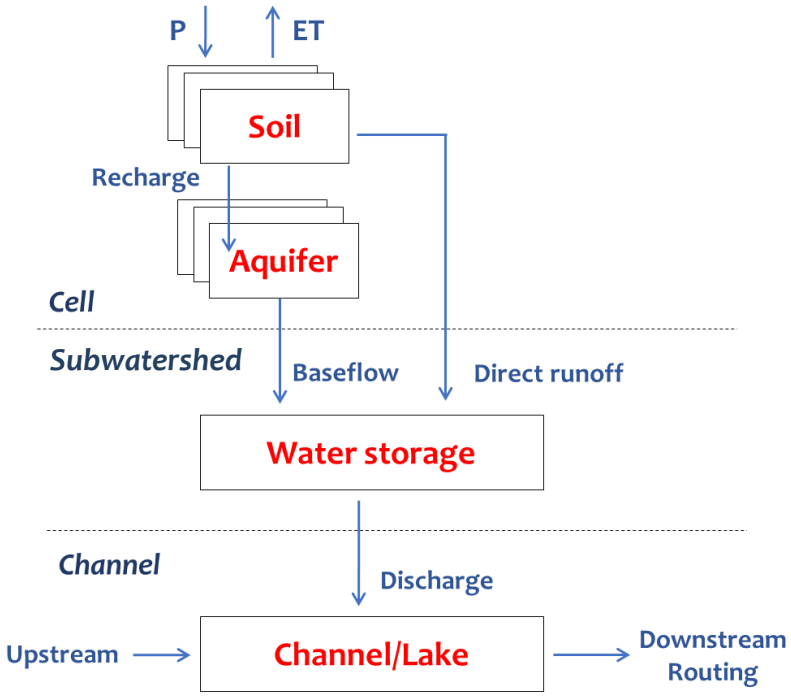

Figure 19. A schematic diagram of the hydrologic processes in REDPOLL

2) Hydrologic processes

○ Precipitation

In REDPOLL, a near-by precipitation monitoring station is assigned to each of the grid cells using the Thiessen polygons around the monitoring stations.

○ Direct runoff

The direct runoff is estimated by using the Curve Number (CN) method suggested by the U.S. Natural Resources Conservation Service (NRCS). In the NRCS-CN method, the direct runoff caused by rainfall is estimated as follows, assuming that the initial abstraction (I_a) is as much as 20% of the potential maximum retention storage (S).

$$Q = \frac{(P - I_a)^2}{(P + 0.8S)} = \frac{(P - 0.2S)^2}{(P + 0.8S)} = \frac{\left[p - (\frac{25400}{CN} - 254)\right]^2}{P + 0.8(\frac{25400}{CN} - 254)}$$

Where, Q = runoff (mm), P= precipitation (mm), CN= runoff curve number, I_a = initial abstraction (mm), S = potential maximum retention storage (mm).

Based on numerous measurements at various watersheds, NRCS derived the relationship between precipitation (P) and direct runoff (Q) as shown in Figure 20 and standardized it to develop a runoff curve number with values between 0 to 100. The following formula demonstrates the relationship between the CN and the potential maximum retention storage of a watershed.

$$\mathrm{CN} = \frac{25{,}400}{S + 254}$$

Even if the same precipitation event occurs at a watershed, the amount of runoff varies depending on the antecedent event of precipitation. Taking this into account, the NRCS-CN method adjusts the CN values according to the Antecedent Moisture Condition (AMC). However, it cannot continuously reflect the changes of AMC and evapotranspiration and the NRCS-CN method has limitations in calculating long-term direct runoff (Boughtons, 1989). To improve this limitation, Williams and Laseur (1976) have developed the Soil Moisture Index (SMI) that can continuously simulate the CN value over time to estimate the continuous long-term surface runoff (Williams *et al*., 2012). REDPOLL adopts the SMI to estimate direct runoff.

Unlike the AMC of the NRCS-CN method, where the potential maximum retention storage (S) falls into three classes, the SMI considers precipitation, evapotranspiration and surface runoff according to the unit of time to continuously estimate S as follows:

$$S_t = S_{t-1} + PET_{t-1} \exp\left(-\frac{BS_{t-1}}{S_{max}}\right) - P_{t-1} + R_{t-1}$$

Where, S_t = retention parameter at the present time step, S_{t-1} = retention parameter at the previous time step, PET_{t-1} = potential evapotranspiration depth at the previous time step, B = depletion coefficient (0~2), S_{max} = maximum value of the retention parameter, P_{t-1} = precipitation depth at the previous time step, R_{t-1} = surface runoff depth.

As presented in the above equation, the SMI methodology allows to continuously estimate direct runoff. In particular, evapotranspiration is an important factor in long-term hydrological losses and should be considered for estimating long-term surface runoff (Ponce and Hawkins, 1996). Penman equation (Penman, 1947) is applied to estimate the potential evapotranspiration (PET) and the NRCS-CN method is applied to estimate surface runoff (R).

The NRCS-CN methodology developed for slopes of 5% has been improved by Wang *et al* (2012), in the APEX model, to adjust the CN value according to the slope. The REDPOLL model takes account of the topography (slope) as follows:

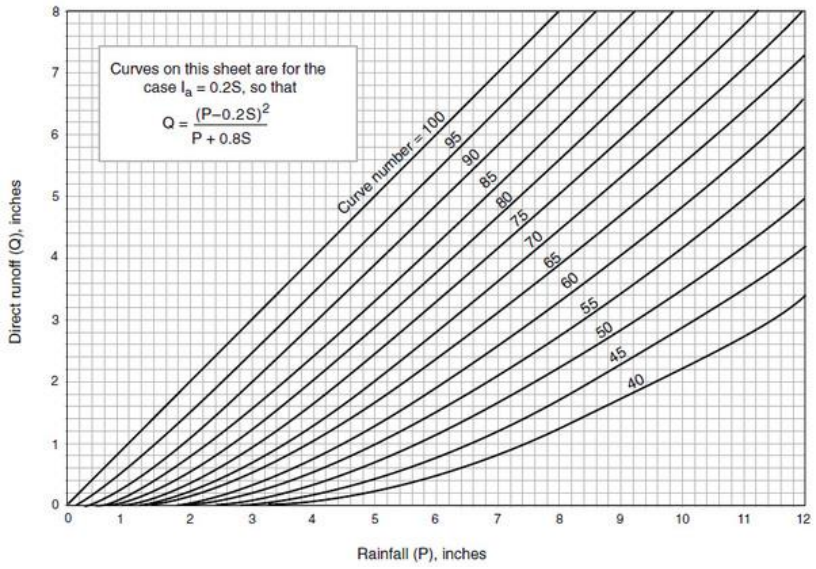

Figure 2013. The Curve-Number (CN) graph of the total direct runoff and precipitation (Cronshey,1986)

$$CN_{2s} = \frac{100}{(1+(\frac{100}{CN_2}-1)\cdot(1.1-\frac{Slp}{Slp+\exp(3.7+0.02117\cdot Slp)}))}$$

Where, CN_2 = Class 2 of AMC of the runoff curve number, Slp = slope (%).

○ Evapotranspiration

Potential retention storage (S) is evapotranspirated and lost to the atmosphere or stored on the surface or infiltrated into the soil. In REDPOLL, evapotranspiration is estimated by adding vegetation transpiration and evaporation from soil (pervious surfaces) and impervious surfaces (Figure 21).

In order to estimate the evapotranspiration, the potential evapotranspiration needs to be estimated first using the Hargreaves equation (Hargreaves and Samani, 1985):

$$PE = 0.0023(R_a/\lambda)T_r^{1/2}(T_a + 17.8)$$

Where, R_a = water equivalent of incoming extra-terrestrial radiation (MJ/m^2/day), T_r = average daily temperature range for a period of days (deg C), T_a = average daily temperature for a period of days (deg C), λ = latent heat of vaporization (MJ/kg) = 2.50 – 0.002361 T_a.

$$R_a = 37.6d_r(\omega_s \sin(\varphi)\sin(\delta) + \cos\varphi)\cos(\delta)\sin(\omega_s)$$

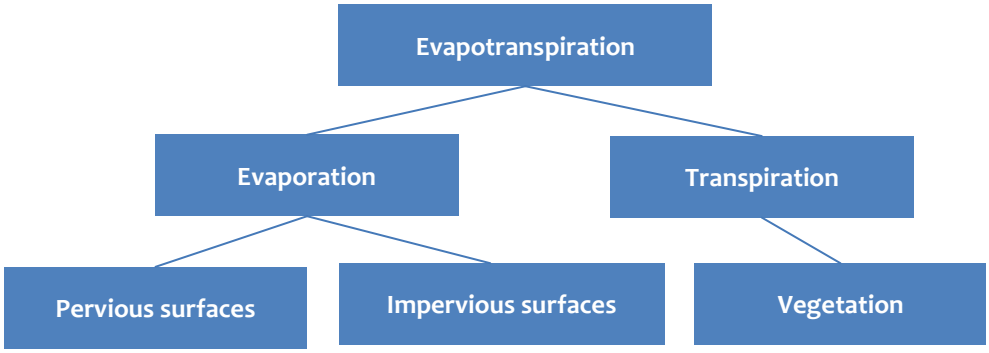

Figure 2114. Estimation of evapotranspiration in REDPOLL

Where, d_r = relative earth-sun distance = 1 + 0.033cos(2πJ/365), J = Julian day (1 to 365), ω_s = sunset hour angle (radians) = $\cos^{-1}$(-tan φ tan δ), φ = latitude (radians), δ = solar declination (radians) = 0.4093 sin (2π(284+J)/365).

Vegetation transpiration is estimated using the equation suggested by Larcher *et al*. (1975) which considers Leaf Area Index (LAI) of the vegetation and soil moisture content:

$$ET = M \cdot \min\left(1, \frac{3}{4}\frac{S_t}{S_{max}}\right) \cdot PE$$

$$M = 1 - e^{-\mu LAI}$$

Where, M = the fraction of soil covered by vegetation, μ = is an extinction coefficient for land cover: 0.35 for grass, 0.45 for crops, 0.5–0.77 for trees (Larcher, 1975), S_t = soil water content at time t, S_{max} = saturated soil water content.

In REDPOLL, the LAI of each vegetation is given as a function of daily average temperature based on the results of Park *et al* (2009)

○ Aquifer recharge and baseflow

Aquifer recharge occurs when soil moisture content is higher than the field capacity. The Eagleson (1978) equation applies soil hydraulic conductivity to estimate aquifer recharge:

$$Q_{rchr} = k_{sat}\left(\frac{S_t}{S_{max}}\right)^{(2+3m)/m}$$

Where, Q_{rchr} = aquifer recharge, k_{sat} = saturated hydraulic conductivity of soil, m = pore-size distribution index, S_t = soil water content at time t, S_{max} = saturated soil water content.

Based on the equation developed by Neitsch *et al*. (2011), in SWAT, baseflow is calculated using the amount of aquifer recharge and the baseflow attenuation coefficient (k_{gwr}) for the soil:

$$Q_{base,\,t} = Q_{base,\,t-1} \cdot exp\left(-k_{gwr}\Delta t\right) + Q_{rchrg,\,t}[1 - \exp\left(\left(-k_{gwr}\Delta t\right)\right]$$

Where, $Qbase_{,t}$ = baseflow on day t (mm/day), $Qbase_{,t-1}$ = baseflow on day t-1 (mm/day), K_{gwr} = baseflow attenuation coefficient (day^{-1}), $Q_{rchrg,t}$ = recharge entering the aquifer on day t.

In REDPOLL, a value of k_{gwr} is designated to each of the sub-watersheds: usually, 0.1 - 0.3 for slow responding sub-watersheds and 0.7 - 0.8 for fast responding sub-watersheds.

○ **Runoff lag in sub-watersheds**

Baseflow and direct runoff from each of the grid cells are aggregated and stored in a virtual water storage for a sub-watershed. Then the water is transported to the outlet of a sub-watershed using a transport function that considers the characteristics of the sub-watershed. A large watershed may have a runoff lag of more than one day and therefore the amount of runoff reaching the watershed outlet on a given day is estimated by considering the time of concentration at the sub-catchment outlets (t_c):

$$Q = (Q' + Q_{stor,t-1}) \cdot (1 - \exp\left[\frac{-k_{lag}}{t_c}\right])$$

Where, Q = direct runoff discharge (mm), Q' = direct runoff generated in a sub-watershed on a given day (mm), k_{lag} = surface runoff lag coefficient, t_c = time of concentration for a sub-watershed (hr).

NRCS (1997) estimates t_c of a catchment as follows:

$$t_c = \frac{1}{1140}\left(\frac{1000}{CN} - 9\right)^{0.7} (3.28084L)^{0.8} S^{-0.5}$$

Where, L = maximum flow distance to a sub-watershed outlet (m), S = sub-watershed mean slope (%), CN = average curve number for a sub-watershed.

3) Estimation of pollution loads

REDPOLL estimates pollution loads of direct runoff and baseflow from each of the grid cells using the event mean concentrations (EMC) measured for a given land use:

$$L_{d,i} = Q_{d,i} \cdot C_{lc,\,i}$$
$$L_{b,i} = Q_{b,i} \cdot C_{cat,\,j}$$

Where, i = cell number, j = sub-watershed number, $L_{d,i}$ = load from direct runoff (kg), $Q_{d,i}$ = direct runoff (m^3), $C_{lc,\,i}$= EMC of direct runoff for each land use, $L_{b,i}$ = load from direct runoff (kg), $Q_{b,i}$ = direct runoff (m^3), $C_{cat,j}$= EMC of baseflow for each sub-watershed.

The EMC of direct runoff is defined for each land use and the EMC of baseflow is defined for each sub-watershed. The EMC for each land use is presented in Table 9.

Pollution loads discharged from each of the grid cells is attenuated during the transport processes including the surface runoff and the river flow processes. The attenuation is estimated according to the flow distance from a given grid cell (also illustrated in Figure 22):

$$L_i = Lo_i \cdot e^{-k_1 L1_{,i}} \cdot e^{-k_2 L2_i}$$

Where, L_i = transported loads from grid cell i (kg), Lo_i = discharged loads from grid cell i (kg), $L1_i$ = surface runoff flow distance from grid cell i to river i (m), $L2_i$ = river flow distance from grid cell i to river i (m), k_1 = surface runoff attenuation coefficient (km^{-1}), k_2 = river flow attenuation coefficient (km^{-1})

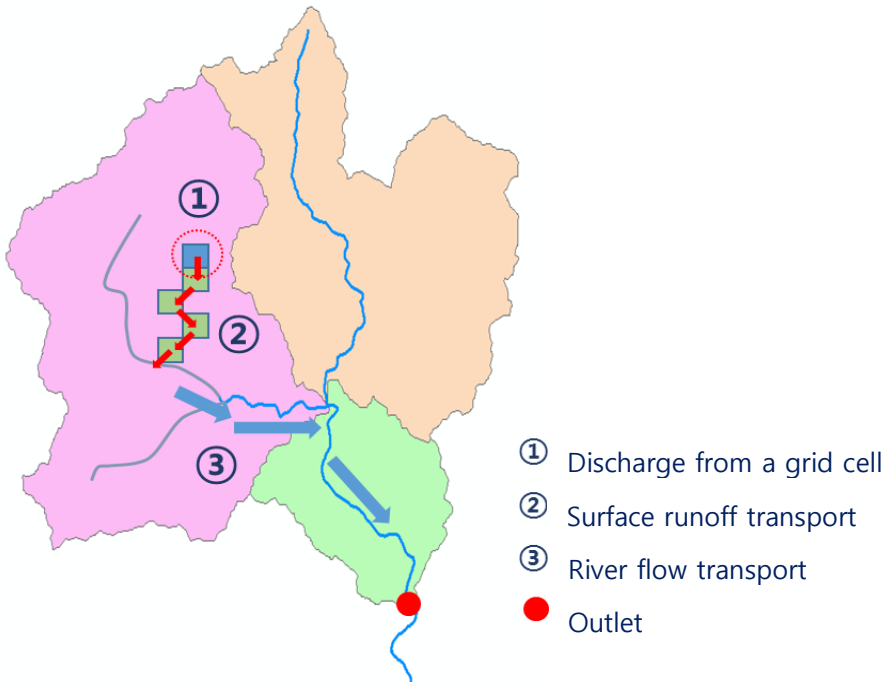

Figure 22. The transport of pollution loads from a grid cell to the watershed outlet

Table 9. EMC of direct runoff for each of the land uses

Land use			EMC (mg/L)		
Primary class	**Secondary class**	**Code**	**BOD**	**TN**	**TP**
Urban/dry area	Residential area	110	5.82	5.04	0.31
	Industrial area	120	19.91	3.63	0.38
	Commercial area	130	34.24	6.95	0.66
	Cultural, sports and leisure area	140	13.03	4.68	0.53
	Roads	150	8.60	3.80	0.24
	Public facilities	160	6.71	5.33	0.34
Agricultural area	Paddy field	210	4.10	2.95	0.41
	Dry field	220	10.75	8.39	2.49
	Orchard	240	3.28	5.69	0.77
	Other cultivation area	250	5.05	7.95	2.66
Forest	Deciduous forest	310	1.48	3.02	0.09
	Coniferous forest	320	1.17	2.25	0.03
	Mixed forest	330	1.29	1.62	0.04
Grassland	Natural grassland	410	5.04	1.55	0.93
	Golf course	421	4.91	8.20	0.86
	Other grassland	423	4.01	3.02	0.31
Bare land	Other bare land	620	8.78	3.85	0.39
	Mining area	621	3.00	0.84	0.06

Previous studies of pollution attenuation rate include studies from Alexander *et al* (2002), Rutherford (2012), Sheibley *et al*. (2015), Keller *et al*. (2014) and Elliott *et al*. (2005) (Table 10). Alexander *et al*. (2002) applied the equation for attenuation process in rivers during the application of the SPARROW model. Based on previous studies, Rutherford (2012) suggested 0.05 km^{-1} as the default value of k for surface runoffs and 0.03 km^{-1} for rivers. A report published by Sheibley *et al*. (2015) applied the RivR-N and Vt models to the Puget Sound Watershed in Washington, United States, to estimate the attenuation coefficient of nutrients (nitrogen and phosphorus) discharged into the river. Keller *et al*. (2014) applied a process-based model to a watershed in Ohio, United States, to estimate total nitrogen (TN) and total phosphorus (TP) attenuation coefficient from the ditch (surface) to the river and in-stream transport. Elliott *et al*. (2005) modified the SPARROW model based on the water quality data from 77 National River Water Quality Network (NRWQN) sites by applying the model to watersheds larger than 10 km^2, in New Zealand. After calibration, the flow rate was classified, based on the results, and attenuation coefficient for each nutrient (N and P) was estimated. As a result, the range of attenuation coefficient for nitrogen and phosphorus was 0.000 km^{-1} ~ 0.3350 km^{-1} and 0.000 km^{-1} ~ 0.1960 km^{-1}, respectively. According to the study, attenuation coefficient had the largest value when the flow rate was low ($Q<0.1$ $m^3 s^{-1}$).

3.2.3 Model set up

The REDPOLL model was set up for the Han River Watershed using square grid cells of 100 m by 100 m and daily time steps for the year 2016. In 2016, the amount of precipitation was similar to that of the average precipitation of the Han River over the last three years (2015 – 2017).

1) Watershed discretization

The REDPOLL model was set up for the Han River Watershed by discretizing it into 49 sub-watersheds (Figure 23). The average area of the 49 sub-watersheds is 702.1 km^2 and the largest sub-watershed is the Imjin-A sub-watershed (Table 11).

2) Node-link networks between sub-watersheds

The node-link networks between the 49 sub-watersheds were set up to simulate river processes (Figure 24). In Figure 24, the yellow boxes indicate those sub-watersheds that have a dam inside.

Table 10. A summary of the attenuation coefficient of water quality parameters proposed by previous studies

Studies	Attenuation coefficient (km^{-1})		
Alexander (2002)	TN	Small streams	0.174~0.223
		Large streams	-0.0001~0.001
	TP	Small streams	0.426~0.430
		Large streams	-0.0006
Rutherford (2012)	Surface		0.0500
	River		0.0300
Sheibley *et al*. (2015)	Nitrate(RivR-N Model)		0.0270
	Nitrate(V_t Model)		0.0480
	Phosphate(V_t Model)		0.0200
Keller *et al*. (2014)	TN	Small rivers	0.0019~0.0160
		Medium rivers	0.0014~0.0120
		Large rivers	0.0004~0.0042
	Surface	TN	0.0040
		TP	0.0200
Elliott *et al*. (2005)	Nitrogen	Flow class 1 ($Q<0.1\ m^3s^{-1}$)	0.3350
		Flow class 2 ($0.1<Q<1\ m^3s^{-1}$)	0.0917
		Flow class 3 ($1<Q<10\ m^3s^{-1}$)	0.0245
		Flow class 4 ($Q>10\ m3s^{-1}$) [a]	0.0000
	Phosphorus	Flow class 1 ($Q<0.1\ m^3s^{-1}$)	0.1960
		Flow class 2 ($0.1<Q<1\ m^3s^{-1}$)	0.0490
		Flow class 3 ($1<Q<10\ m3s^{-1}$) [a]	0.0000

[a] Adjusted attenuation coefficient to not go below 0

Figure 23. The 49 sub-watersheds of the Han River Watershed

Table 11. A statistical summary of the 49 sub-watersheds of the Han River Watershed

Category	Area (km^2)	Name
Maximum	4,236.3	Imjin-A
Minimum	134.9	Gulpo-A
Average	702.1	-
Median	468.7	North Korea-C

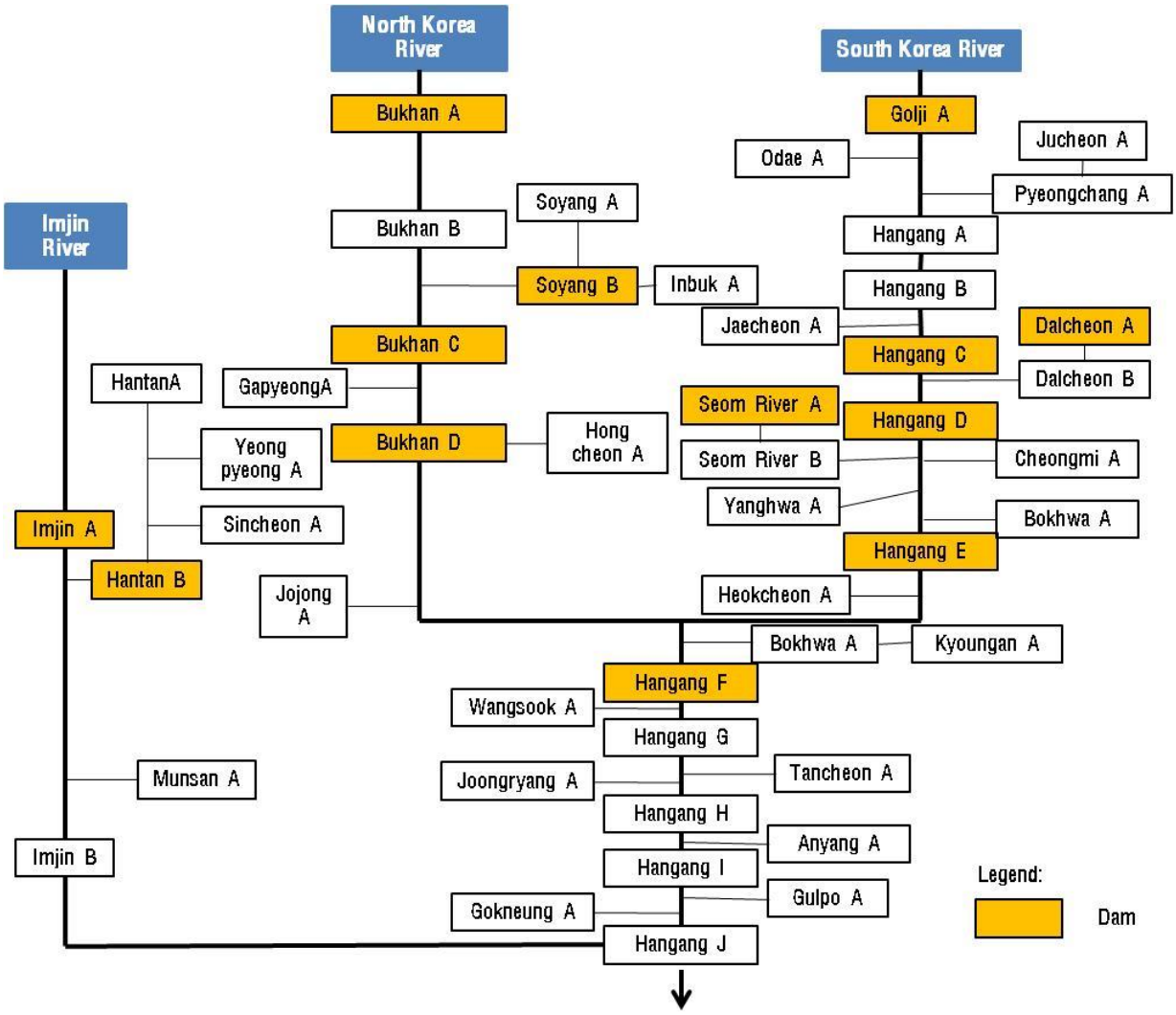

Figure 2415. A schematic diagram of node-link networks between the 49 sub-watersheds of the Han River Watershed

3) Input data

The REDPOLL model requires various spatio-temporal data including weather, topography, land cover, vegetation, soil, aquifer, point sources, river network, and the map of the total maximum daily load management programs (TMDLMP) watersheds (Table 12).

Table 12. List of the input data required for setting up the REDPOLL model

Data type	Description/properties	Source
Weather	Precipitation, temperature	Korea Meteorological Administration
Topography	Elevation, slope, flow direction, flow accumulation	National Geographic Information Institute, RO Korea
Land cover	Land cover classification	Land cover classification of the Ministry of Environment, USGS
Vegetation	Leaf Area Index (LAI)	Land cover classification of the Ministry of Environment, RO Korea
Soil	Soil moisture content, saturated hydraulic conductivity, soil porosity distribution index	Detailed soil map of National Institute of Agricultural Sciences, RO Korea
Aquifer	Baseflow attenuation coefficient (k_{grw})	-
Point sources	Treated and untreated point-sources	Pollution source investigation data of the Ministry of Environment, RO Korea
River network	National rivers, local streams, river/stream width and depth	National Geographic Information Institute, RO Korea
TMDLMP map	Map of the TMDLMP watersheds	Ministry of Environment, RO Korea

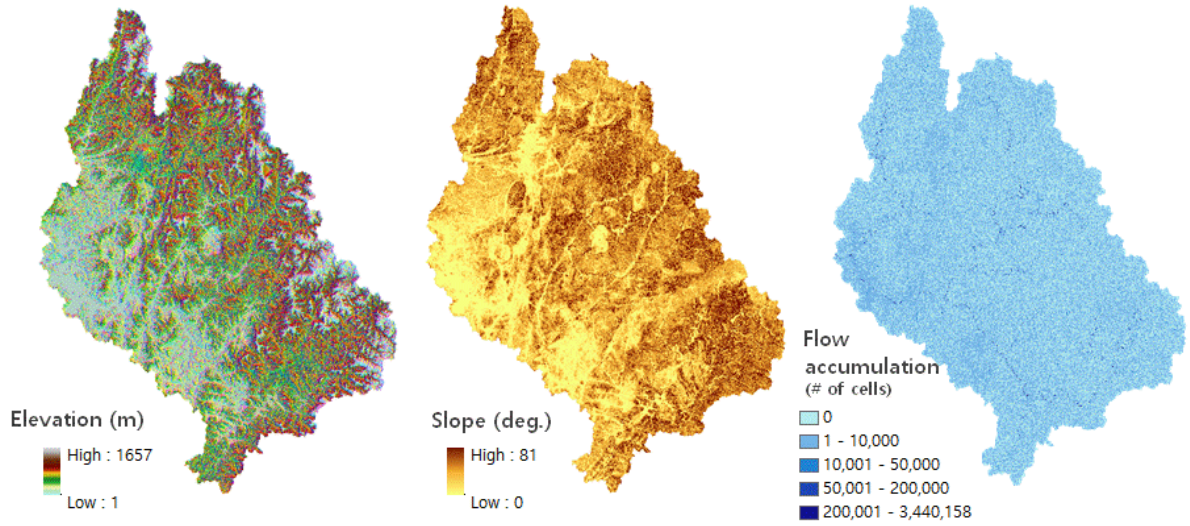

Figure 2516. Topographic analyses of the study area: elevation, slope and flow accumulations

○ Topography

Estimation of the surface slope, flow directions and flow accumulations was carried out using DEM of the Han River Watershed. The maximum elevation of the ground within the Han River Watershed is 1,657 m and the maximum slope is 81° (Figure 25).

○ Land cover

Land cover of the Han River Watershed was set up using the national land cover data set provided by the Ministry of Environment. As the DPR Korean territory within the Han River Watershed is not covered by the national data set, the global land cover data set from the 500 m MODIS satellite images provided by the USGS was used to fill the land cover of the DPR Korean areas.

Forest and agriculture is dominating the land cover of the Han River Watershed (Figure 26). Forest covers 66.5%, agricultural area covers 25% and urban area covers 4.3% of the total area of the Han River Watershed (Table 13). The LAI (leaf area index) was estimated using a temperature function to consider seasonal variation, as proposed by Park *et al*. (2009).

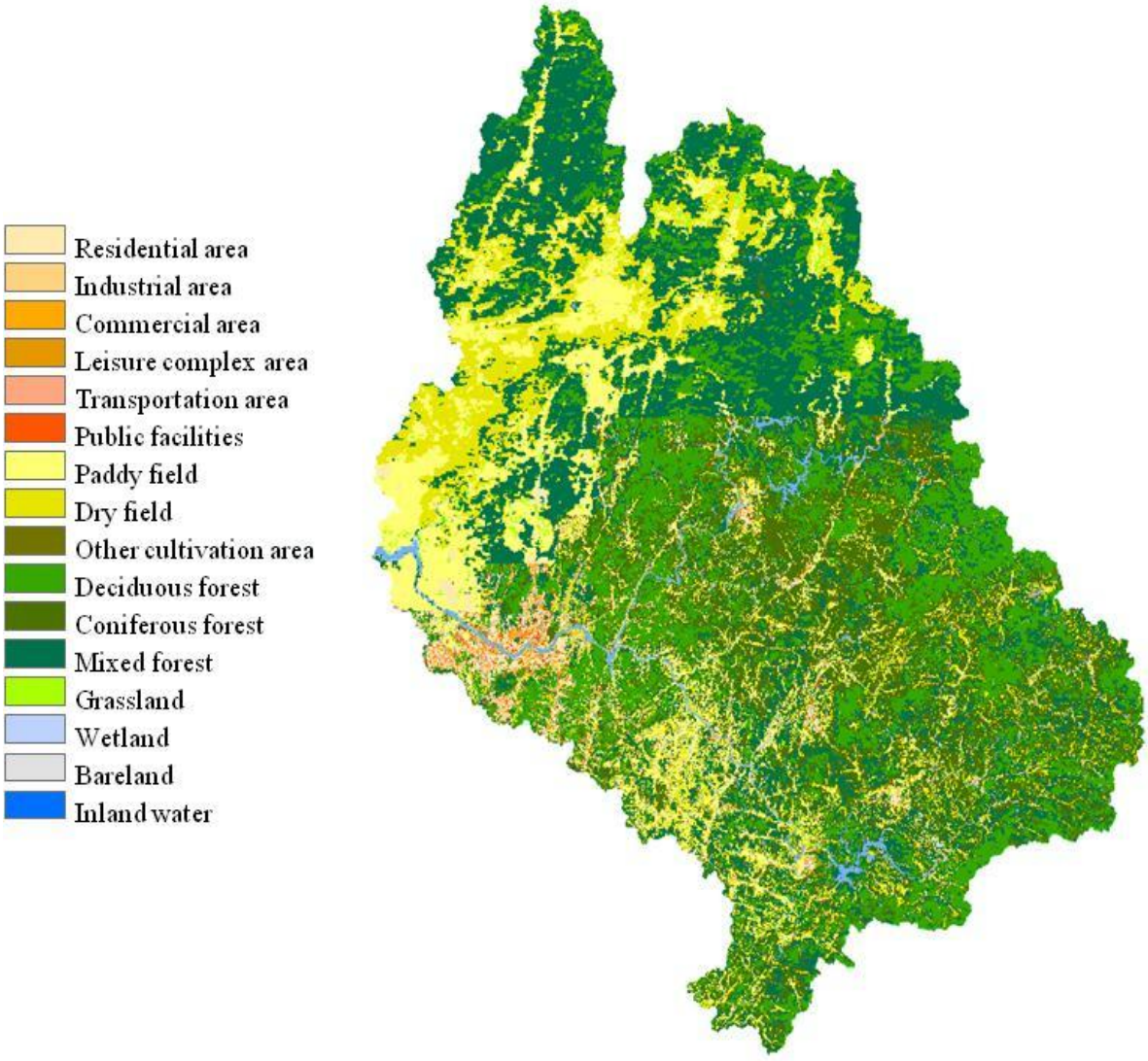

Figure 26. Land cover of the Han River Watershed

Table 13. Land uses in the Han River Watershed

Land use	Area (km^2)	Area ratio (%)
Residential area	814.7	2.4
Industrial area	123.2	0.4
Commercial area	123.7	0.4
Leisure complex area	18.0	0.1
Roads	214.6	0.6
Public facilities	154.7	0.4
Paddy field	3839.4	11.2
Dry field	4572.4	13.3
Other cultivation area	165.7	0.5
Deciduous forest	6516.2	18.9
Coniferous forest	6752.8	19.6
Mixed forest	9638.1	28.0
Grassland	312.24	0.91
Wetland	366.57	1.07
Bare land	288.89	0.84
Inland water	500.37	1.45
Total	34401.6	100.0

○ **Soil texture**

Direct runoff is highly influenced by soil infiltration. In general, the higher the soil infiltration the lower the direct runoff and vice versa. Based on the NRCS-CN method, any soil falls into one of the four Hydrologic Soil Groups (HSGs) according to the soil infiltration rate (Table 14).

The HSGs in the Han River Watershed is shown in Table 15 and Figure 27. The HSGs data from the National Institute of Agricultural Sciences(NIAS) was used for the RO Korean territory. As for the DPR Korean territory within the Han River Watershed where the NIAS soil data base is unavailable, the entire area was classified as HSG B based on the global soil data from the

Harmonized World Soil Database (Figure 27). The HSG A and HSG B covers 44.7% and 42.0%, respectively, of the total area of the watershed (Table 15).

In the Han River Watershed, sandy loam and loam respectively covers 50.8% and 29.6% of the total watershed area (Figure 28 and Table 16). The soil physical parameters such as the soil water content and the saturated hydraulic conductivity was set up for the REDPOLL model (Table 17).

Table 14. Soil infiltration rate for the Hydrologic Soil Groups (HSGs)

HSG	Minimum infiltration rate (in/hr)	Remarks
A	0.30~0.45	Fast
B	0.15~0.30	Average
C	0.05~0.15	Slow
D	0.00~0.05	Very slow

Table 15. The HSGs in the Han River Watershed

HSG	Area (km^2)	Proportions (%)
A	15384.9	44.7
B	14451.2	42
C	2418.3	7
D	2147.3	6.2
Total	34401.6	100

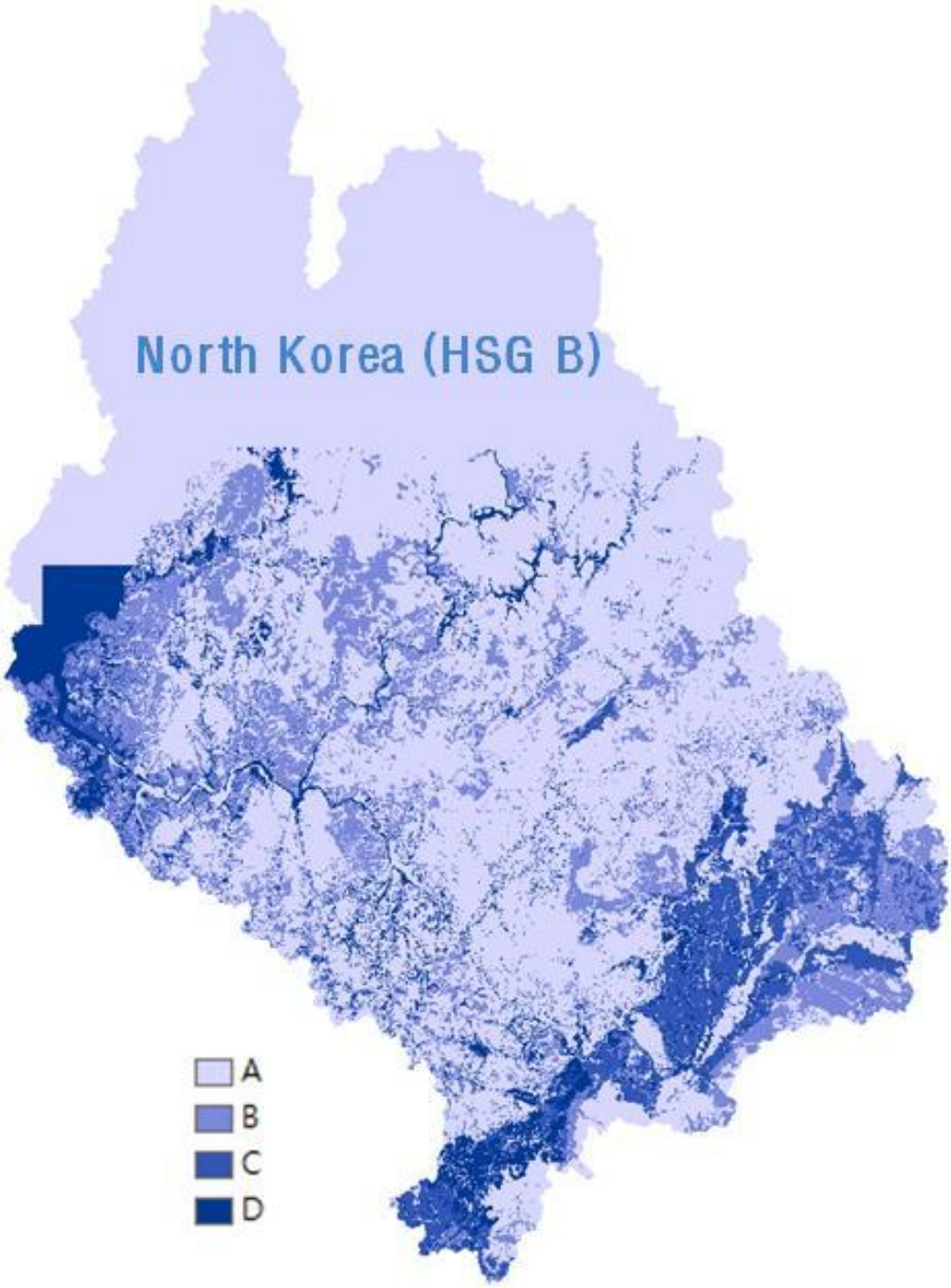

Figure 2717. Spatial distribution of the HSGs in the Han River Watershed

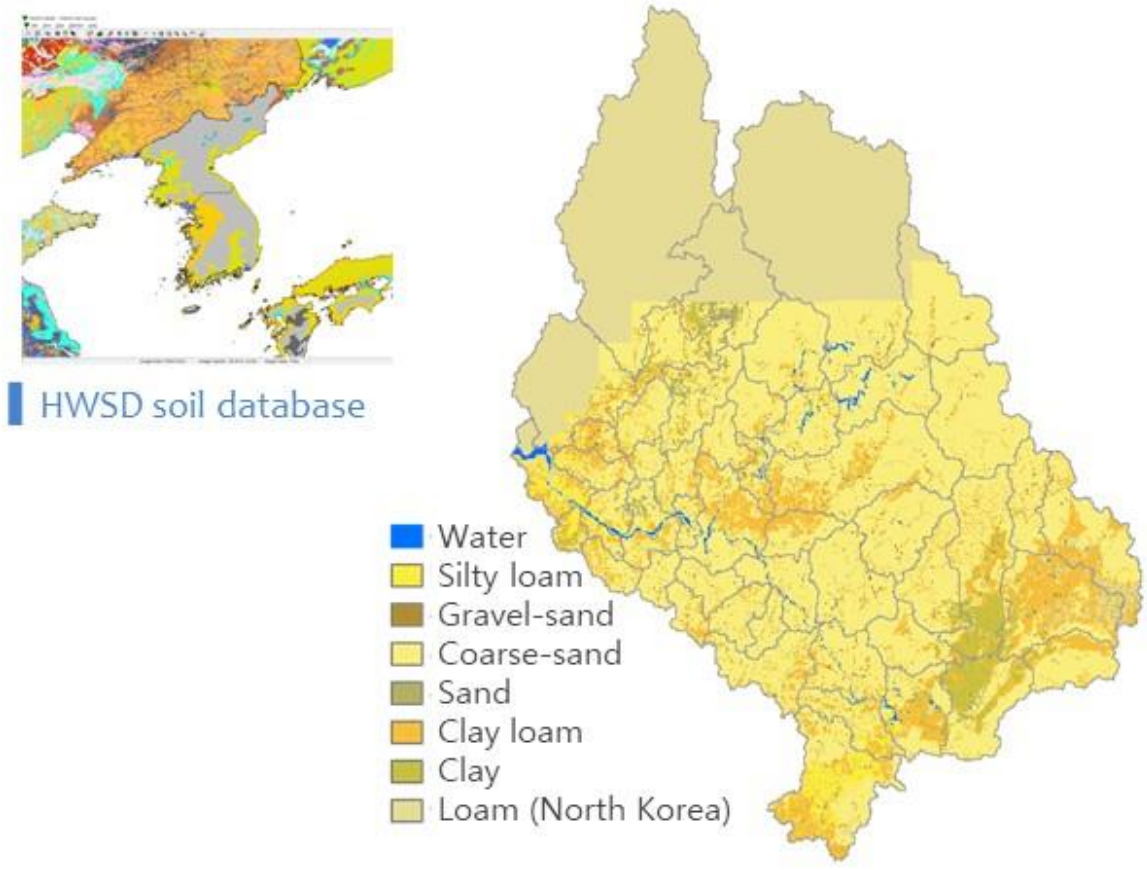

Figure 28. Spatial distribution of soil textures in the Han River Watershed

Table 16. Soil textures in the Han River Watershed

Soil Texture	Area (km^2)	Proportions (%)
Water	215.2	0.6
Silty loam	734.8	2.1
Gravel	239.2	0.7
Sandy loam	17465.4	50.8
Sand	236.8	0.7
Clay loam	4302.3	12.5
Clay	1019.6	3.0
Loam	10188.3	29.6
Total	34401.6	100.0

Table 17. Soil physical parameter values set for the REDPOLL model

Soil Texture	Soil water content at saturation (m^3/m^3)	Soil water content at field capacity (m^3/m^3)	Saturated hydraulic conductivity (m/day)	Pore-size distribution index
Silty loam	0.486	0.330	0.209	0.234
Gravel	0.500	0.091	6.500	0.720
Sandy loam	0.453	0.207	1.455	0.378
Sand	0.437	0.091	4.657	0.694
Clay loam	0.460	0.318	0.102	0.242
Clay	0.480	0.396	0.045	0.165
Loam	0.463	0.270	0.232	0.252

○ **Flow distance**

Pollution loads from grid cells are transported to the outlet of the watersheds. The attenuation of the pollution loads is estimated using the flow distance of the surface runoff, headwaters and rivers. The flow distance is estimated from spatial analyses of the Han River Watershed topographic data (Figure 29).

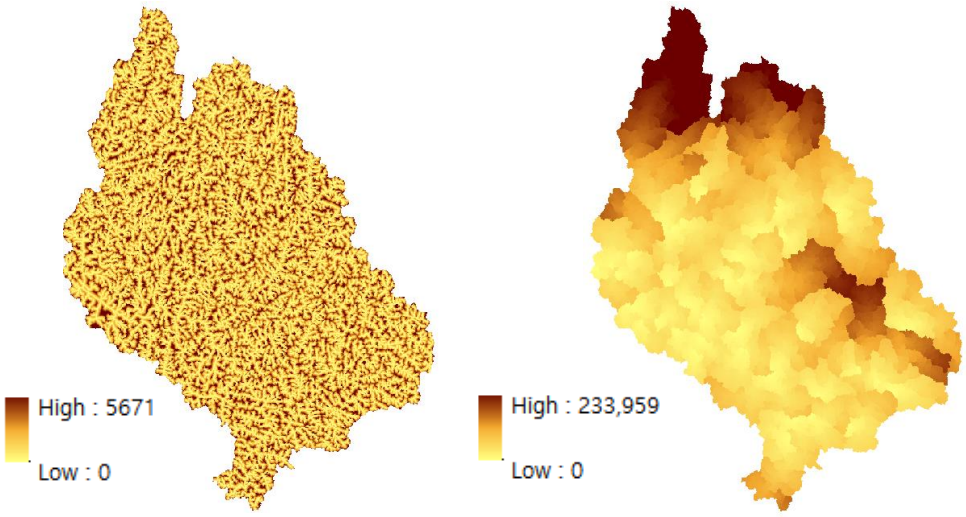

(a) Flow distance of surface runoff and headwaters (m) **(b) Flow distance of the rivers (m)**

Figure 189. The estimated flow distance in the Han River Watershed

○ **Weather data**

The daily precipitation and temperature (max, min and mean) data were collected from 18 weather stations within the Han River Watershed (Figure 30). The near-by weather stations were assigned to each of the 49 sub-watersheds by using the Thiessen polygons approach.

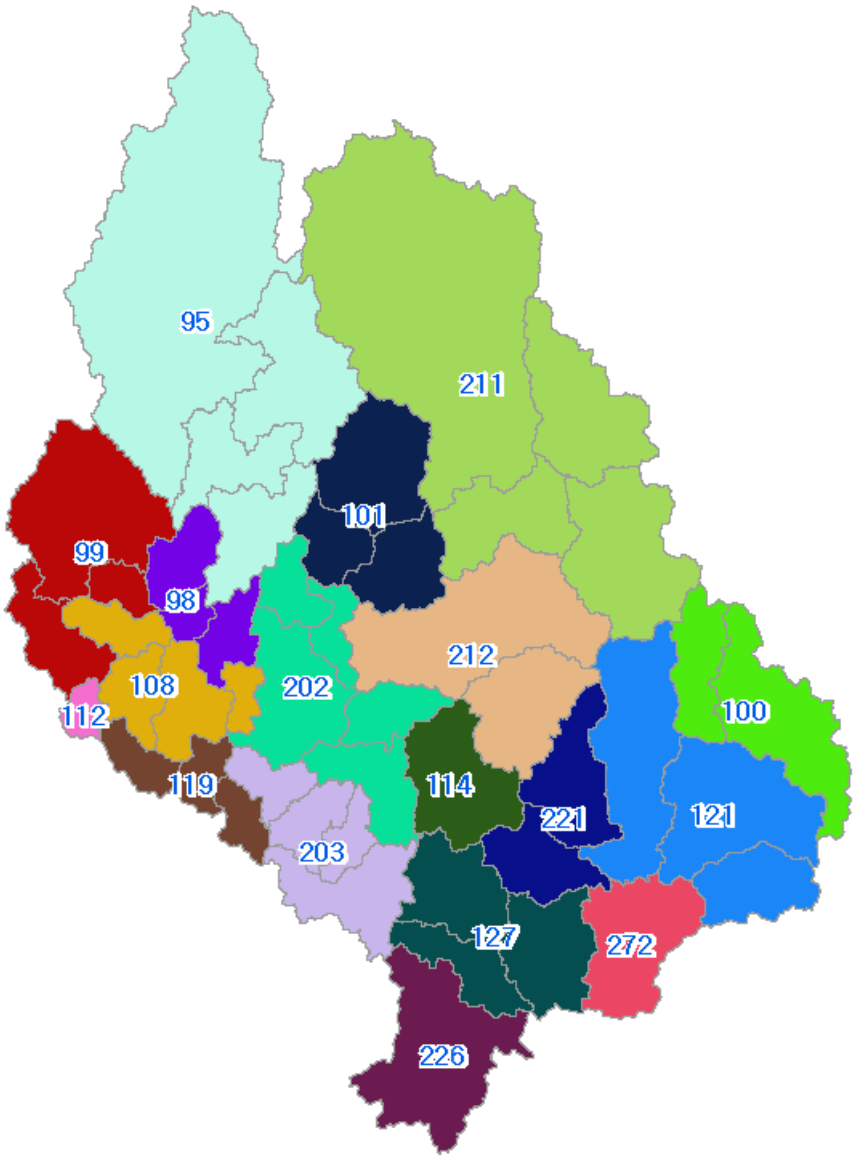

Figure 3019. The 18 weather stations and the 49 sub-watersheds within the Han River Watershed

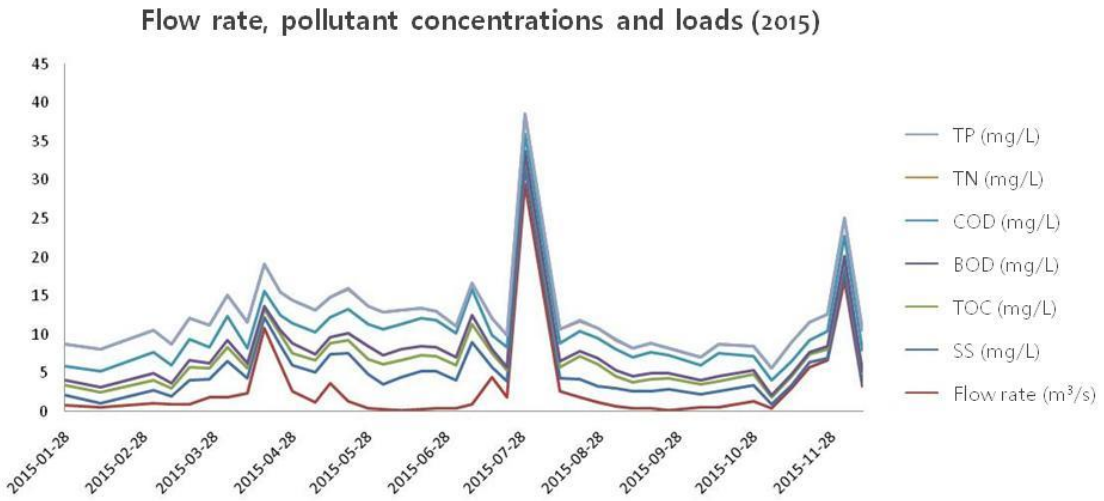

Figure 31. The observed flow rate and water quality parameters

○ **Observed flow rate and water quality**

The observed flow rate and water quality data were collected for model calibration. The flow rate and water quality data were monitored every 8 days under the Total Maximum Daily Load Management Programs at the outlets of the 49 sub-watersheds. These data were used for model calibration (Figure 31).

○ **Point-source discharges**

Using the observed discharge data from sewage treatment plants, provided by the Ministry of Environment, the point source discharges were set for the 49 sub-watersheds of the River Han Watershed. The observed discharge data includes flow rate, BOD, COD, SS, TN and TP.

○ **Abstractions and discharges from dams**

The abstractions and water quality data from the 15 major dams within the Han River Watershed were collected and used for model set up. The average monthly amount of abstraction and water quality were estimated using the observed data from 2013 to 2017.

Dam discharges were evaluated using the non-linear regression equations derived from the observed water storage ratio, inflows, and precipitations of the upstream watershed. Table 18 shows the correlation analysis results between the observed and the estimated discharges and Figure 32 illustrates scatter plots of observed and estimated discharges for the Yipo Dam and the Soyang Dam.

Table 18. The R^2 values of the correlations between the observed and the estimated discharges of some major dams in the River Han Watershed

Name	R^2	Name	R^2
Guangdong Dam	0.57	Gunnam Dam	0.99
Peace Dam	0.99	Chungju Dam	0.62
Chuncheon Dam	0.99	Yipo Dam	0.99
Cheongpyeong Dam	0.99	Paldang Dam	0.99
Soyang Dam	0.62	Hantan Dam	0.98

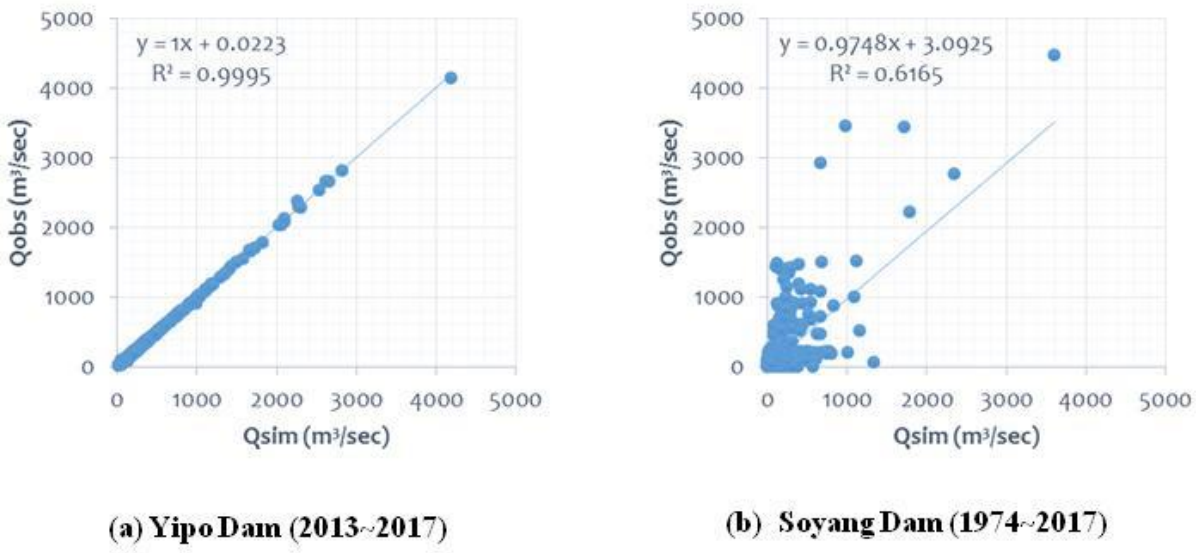

(a) Yipo Dam (2013~2017)

(b) Soyang Dam (1974~2017)

Figure 32. Scatter plots of the observed and the estimated dam discharges

4) Evaluation of model accuracy

Model calibration was performed for the 48 sub-watersheds. The Han River-J sub-watershed, located at the outlet of the Han River Watershed, was excluded for model calibration as the river flow and water quality data are likely affected by the coastal tides. The river flow and water quality data observed on every 8 days can demonstrate seasonal variation in general but cannot present the effects of rainfall events in detail. Considering this limitation in the observed data, the accuracy of the model was evaluated using PBIAS (Percent BIAS, %).

PBIAS measures the average tendency of the simulated values to be larger or smaller than their observed values. The optimal value of PBIAS is 0.0, with low-magnitude values indicating accurate model simulation. Positive values indicate overestimation bias, whereas negative values indicate underestimation bias. PBIAS can be calculated using the following equation (Gupta *et al*., 1999):

$$PBIAS = \frac{\left|\sum_{i=1}^{n} O_i - \sum_{i=1}^{n} P_i\right|}{\sum_{i=1}^{n} O_i} \times 100$$

Where, O_i = observed data, P_i = simulated data, n = number of simulation and observation.

Moriasi *et al*. (2007) proposed the following PBIAS criteria for the monthly simulation results of watershed models:

- Flow rate: Very good ±10%, Good ±15%, Satisfactory ±25%
- Water quality: Very good ±25%, Good ±40%, Satisfactory ±70%

3.3 Results and Discussion

3.3.1 Model calibration

1) River flows

The flow-related parameters including CN values (adjusted between -20% to +20% of the standard value), watershed lag coefficient (K_{lag}), and baseflow recession coefficient (K_{gwr}) were adjusted for model calibration. The flow rate calibration results for each of the 48 sub-watersheds are illustrated in Figure 33. The PBIAS values of the flow rate ranges between 0.4% and 135.6% (average 28.5%). Given that the monitoring data are discontinuous, observed only on every 8 days, the calibration results are considered to be fairly reasonable. The average PBIAS and R^2 values of flow rates for the five continuous monitoring stations showed a satisfactory level of 16.03% and 0.68, respectively (Table 19).

Figure 34 and Figure 35 illustrate the simulated and the observed flows at the Odae-A Station and the Han River-H Station. The simulated flows were either under-estimated or over-estimated to some extent, but it is certain that the calibrated model simulates daily and seasonal variation of river flows reasonably.

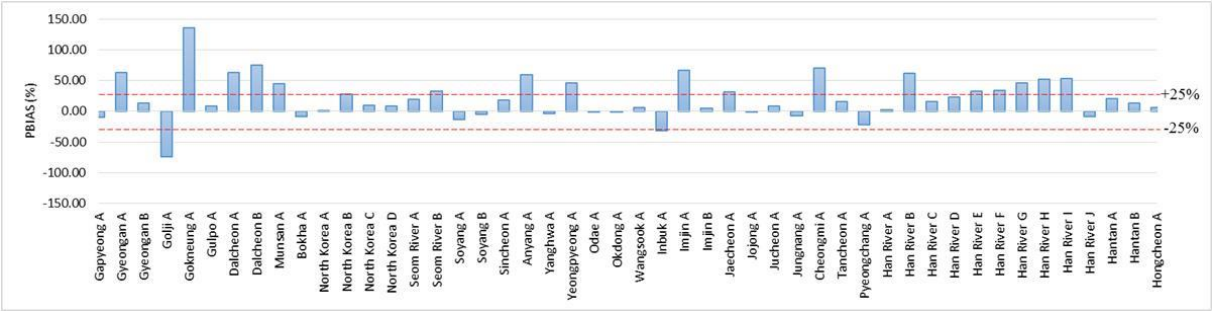

Figure 33. The PBIAS values of the flow rates for each of the 48 sub-watersheds

Table 19. The PBIAS and R^2 values of the flow rates at the five continuous monitoring stations within the Han River Watershed

Name	PBIAS(%)	R^2
Odae-A	-1.47	0.53
PyeongChang-A	-22.01	0.75
Han River-A	3.01	0.85
Han River-H	47.91	0.77
Heukcheon-A	5.73	0.49
Average (Absolute value)	16.03	0.68

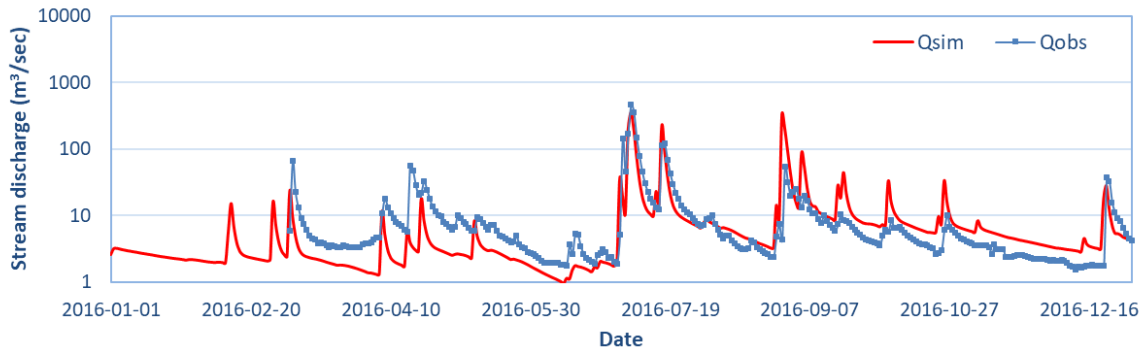

Figure 34. The simulated and the observed flows at the Odae-A Station

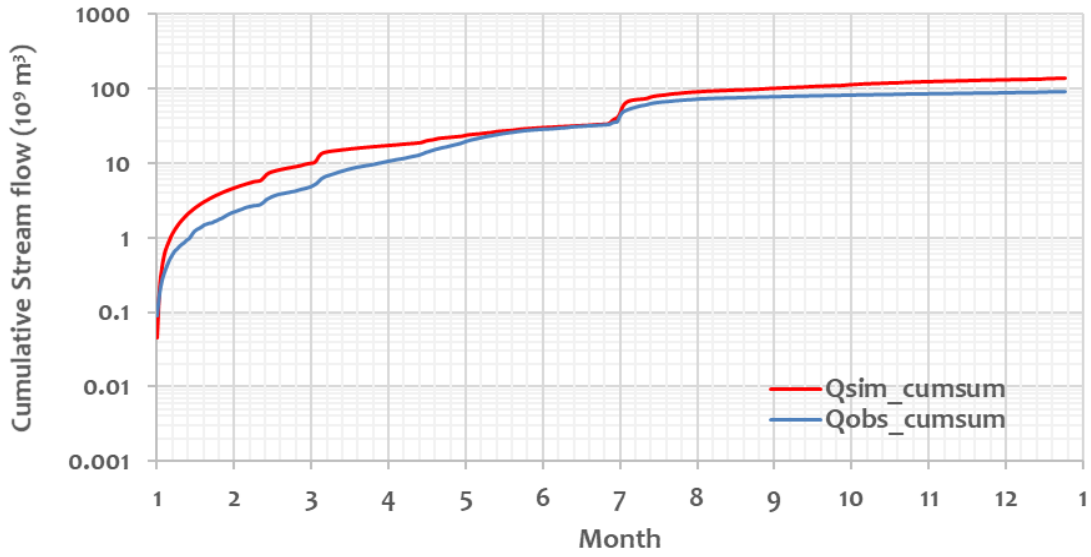

Figure 35. The simulated and the observed cumulative flows at the Han River-H Station

2) Water quality

The water-quality related parameters including EMC values (adjusted between -50% to +50% of the standard value) and attenuation coefficient (adjusted within the range of values given from previous studies) were adjusted for model calibration. As presented in Table 20 and Figure 36, the PBIAS values of the water quality parameters for the 48 sub-watersheds vary in a wide range: SS -76.9% and 201.0% (average 66.8%); BOD -54.9% and 143.0% (average 30.5%); TN -44.6% and 153.4% (average 21.0%); and TP -79.8% an 196.5% (average 53.2%). Given that the monitoring data are discontinuous, the calibration results are considered to be fairly reasonable.

Table 20. A statistical summary of the calibration results, PBIAS (%), for each of the water quality parameters

	SS	BOD	TN	TP
Maximum	201.0	143.0	153.4	196.5
Minimum	-76.9	-54.9	-44.6	-79.8
Average (Absolute value)	66.8	30.5	21.0	53.2
Rating[(1)]	Satisfactory	Good	Very good	Satisfactory

(1) Moriasi *et al*. (2007)

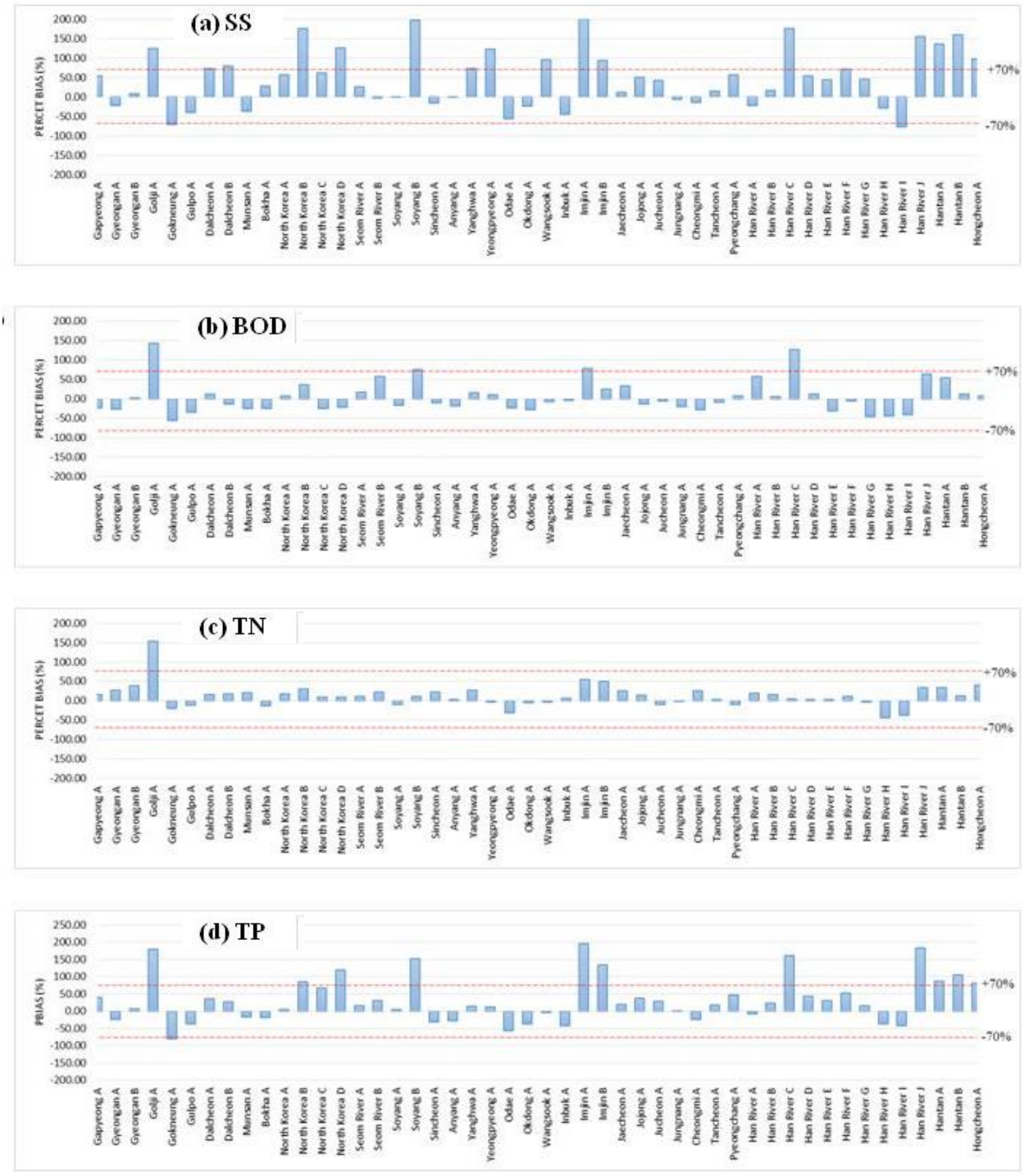

Figure 36. The PBIAS values of water quality parameters for each of the 48 sub-watersheds

3.3.2 Water flows and water balance

1) Daily and monthly flows

As illustrated in Figure 37, the temporal variation of daily flows from the Han River Watershed to the Yellow Sea is very large: the daily maximum flow of 1,409.9 x 10^6 m^3/day is 278 times larger than the daily minimum flow of 6.2 x 10^6 m^3/day (average 58.2 x 10^6 m^3/day). The monthly flows show also a large temporal variation as shown in Table 21 and Figure 38. The total annual flow to the Yellow Sea from the Han River Watershed in 2016 is estimated as 21,285.9 x 10^6 m^3/year. The monthly maximum flow of 7,483.7 x 10^6 m^3/month in July is almost 12 times greater than the monthly minimum flow of 634.4 x 10^6 m^3/month in June. Resultantly, 35.2% of the annual total flow from the Han River Watershed flows to the Yellow Sea in July. These figures will vary from year to year but it is very likely that the temporal variation of daily and monthly flows to the Yellow Sea will remain very large as far as the monsoon weather system affects the region.

Table 21. Monthly flows to the Yellow Sea from the Han River Watershed in 2016

Month	Precipitation (mm/month)	Flow (10^6 m^3/month)	Proportions of monthly flow (%)
January	10.7	773.1	3.6
February	47.7	927.7	4.4
March	38.7	1,182.4	5.6
April	91.9	871.6	4.1
May	107.1	1,301.8	6.1
June	34.1	634.4	3.0
July	**442.9**	**7,483.7**	**35.2**
August	77.9	1,611.8	7.6
September	52.4	1,509.8	7.1
October	119.6	2,498.1	11.7
November	17.1	1,124.3	5.3
December	59.4	1,367.2	6.4
Total	1100.6	**21,285.9**	100.0

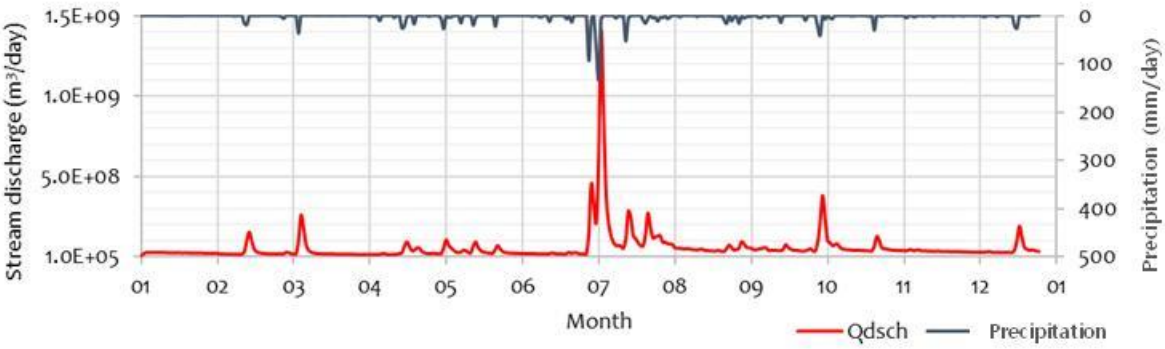

Figure 37. The temporal variation of daily flows to the Yellow Sea from the Han River Watershed in 2016

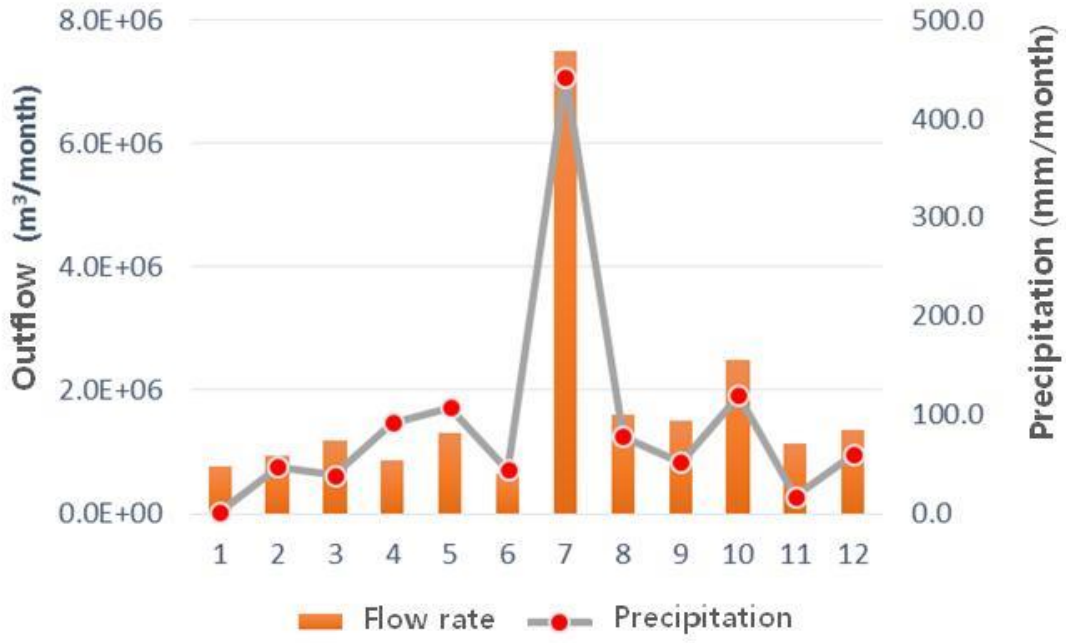

Figure 38. The temporal variation of monthly flows to the Yellow Sea from the Han River Watershed in 2016

2) **Water balance**

The model simulation was carried out for the year 2016 and the water balance for the Han River Watershed is presented in Table 21. In 2016, there was a total precipitation of 1,100.6 mm/year in the Han River Watershed. The evapotranspiration was 456.4 mm/year and the river flow was 629.2 mm/year accounting for 41.5% and 57.2% of the total precipitation, respectively. It was estimated that the river flow to the Yellow Sea was 618.7 mm accounting for 56.2% of the total precipitation. The direct runoff and baseflow respectively accounted for 35.9% and 21.2% of the total precipitation.

Table 22. Estimated water balance for the Han River Watershed in 2016

	Hydrological Processes	**mm/year**	**%**
Inflow	Precipitation	1100.6	100.0
	Discharge from point-sources	70.9	6.4
Outflow	Evapotranspiration	456.4	41.5
	Transpiration	(271.7)	(24.7)
	Soil evaporation	(181.2)	(16.5)
	Impervious surface evaporation	(3.5)	(0.3)
	Abstraction	45.8	4.2
	River flow to the Yellow Sea	618.7	56.2
	Direct runoff	(395.6)	(35.9)
	Baseflow	(233.6)	(21.2)
Storage change		50.5	4.7

3.3.3 Pollution loads

1) Daily and monthly pollution loads

The temporal variation of daily pollution loads to the Yellow Sea from the Han River Watershed in 2016 is very large as shown in Table 23 and Figure 39. The daily maximum SS load of 95,508.5 ton/day is 3,673 times larger than the daily minimum SS load of 26.0 ton/day (average 2,285.6 ton/day). As for other pollutants, the daily maximum loads are BOD 4,641.3 ton/day, TN 4,730.9 ton/day, TP 352.4 ton/day, the daily average loads are BOD 153.4 ton/day, TN 225.5 ton/day, TP 10.4 ton/day, and the daily minimum loads are BOD 25.9 ton/day, TN 62.4 ton/day, TP 1.4 ton/day.

The monthly pollution loads show also a large temporal variation as presented in Table 24 and Figure 40. The total annual pollution loads to the Yellow Sea from the Han River Watershed in 2016 is estimated as SS 836,546.4 ton/year, BOD 56,143.3 ton/year, TN 82,543.8 ton/year, and TP 3,788.3 ton/year. The monthly maximum SS load of 413,311.5 ton/month in July is about 225 times greater than the monthly minimum SS load of 1,838.4 ton/month in January, contributing almost half (49.4%) of the annual total load to the Yellow Sea. As for other pollutants, the monthly maximum loads are BOD 22,485.0 ton/month, TN 25,498.0 ton/month, TP 1,575.9 ton/month in July, and the monthly minimum loads are BOD 1,386.7 ton/month in January, TN 3,237.1 ton/month in June, TP 66.4 ton/month in June.

The above figures will vary from year to year but it is very likely that the temporal variation of daily and monthly flows to the Yellow Sea will remain very large as far as the monsoon weather system affects the region.

Table 23. A statistical summary of the daily pollution loads to the Yellow Sea from the Han River Watershed in 2016

	SS		BOD		TN		TP	
	Loads (ton/day)	Ratio to Min	Loads (ton/day)	Ratio to Min	Loads (ton/day)	Ratio to Min	Loads (ton/day)	Ratio to Min
Max	95,508.5	3,673.4	4,641.3	179.2	4,730.9	75.8	352.4	251.7
Min	26.0	1.0	25.9	1.0	62.4	1.0	1.4	1.0
Average	2,285.6	87.9	153.4	5.9	225.5	3.6	10.4	7.4

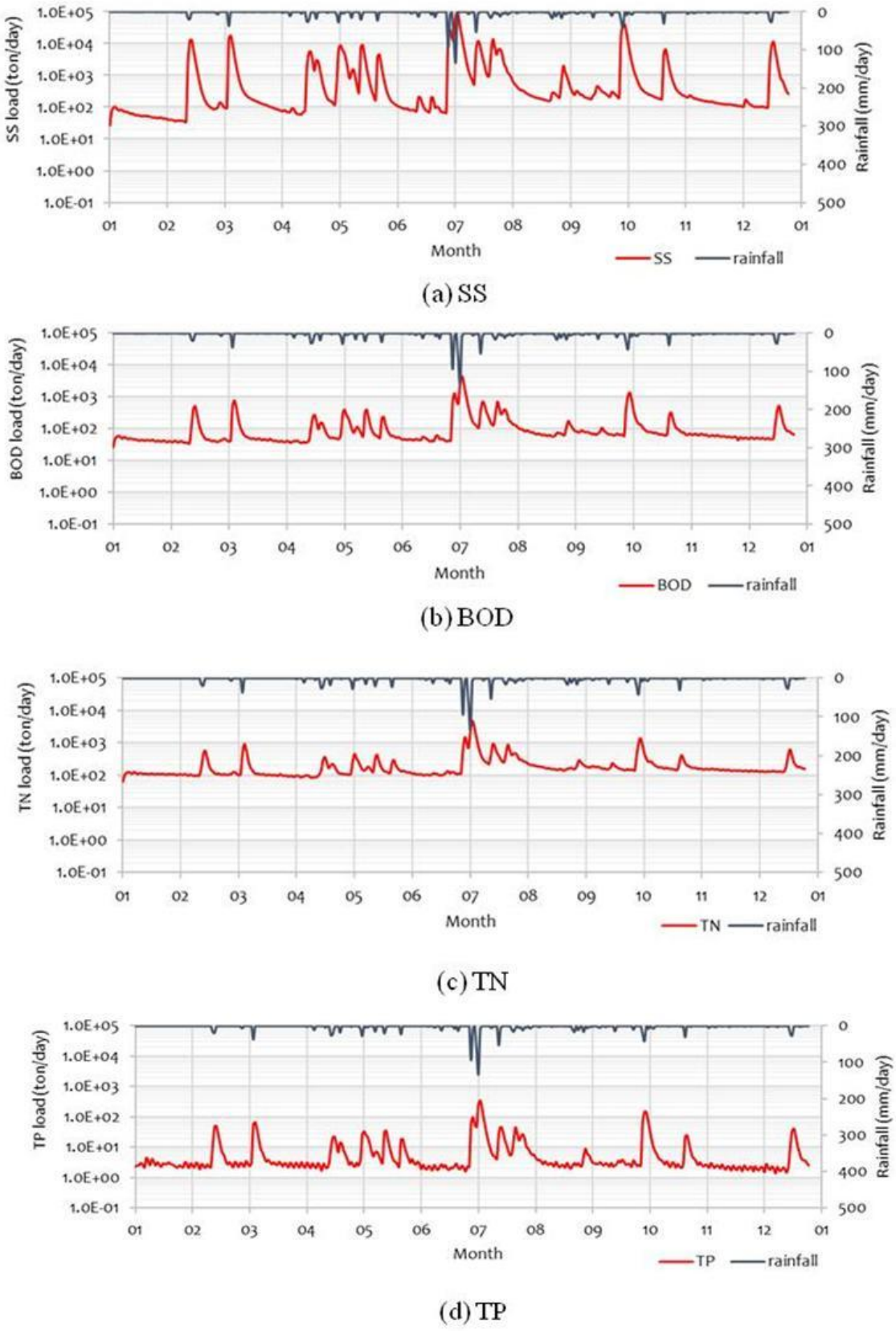

Figure 39. The temporal variation of daily pollution loads to the Yellow Sea from the Han River Watershed in 2016

Table 24. Monthly pollution loads to the Yellow Sea from the Han River Watershed in 2016

Month	SS		BOD		TN		TP	
	(tons)	(%)	(tons)	(%)	(tons)	(%)	(tons)	(%)
January	1,838.4	0.2	1,386.7	2.5	3,541.7	4.3	84.2	2.2
February	40,722.3	4.9	2,523.2	4.5	4,263.6	5.2	217.8	5.8
March	52,472.7	6.3	3,325.7	5.9	5,033.5	6.1	266.0	7.0
April	27,079.0	3.2	2,252.4	4.0	3,831.3	4.6	164.0	4.3
May	74,915.6	9.0	4,087.4	7.3	5,637.1	6.8	340.0	9.0
June	3,127.3	0.4	1,417.0	2.5	3,237.1	3.9	66.4	1.8
July	413,311.5	49.4	22,485.0	40.0	25,498.0	30.9	1,575.9	41.6
August	12,534.0	1.5	2,971.1	5.3	5,897.3	7.1	104.3	2.8
September	11,637.0	1.4	2,803.4	5.0	5,503.5	6.7	97.3	2.6
October	156,841.5	18.7	7,545.7	13.4	9,850.8	11.9	624.1	16.5
November	5,256.6	0.6	2,018.1	3.6	4,494.0	5.4	67.3	1.8
December	36,810.5	4.4	3,327.7	5.9	5,755.8	7.0	181.0	4.8
Total	836,546.4	100.0	56,143.3	100.0	82,543.8	100.0	3,788.3	100.0

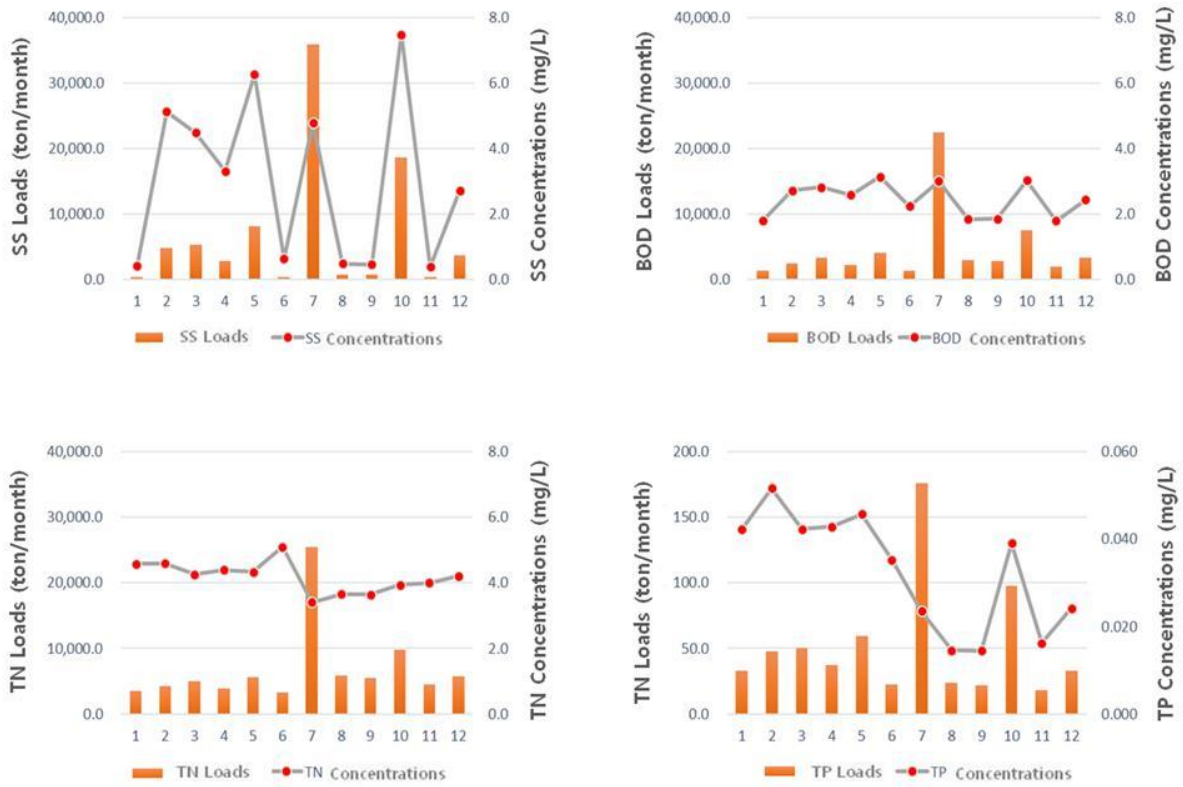

Figure 40. The temporal variation of monthly pollution loads to the Yellow Sea from the Han River Watershed in 2016

2) Sources of pollution loads

For effective management of a watershed, it is critical to understand the proportions of pollution loads from each type of sources. Based on the REDPOLL simulations, the sources and their pollution loads to the Yellow Sea from the Han River Watershed in 2016 are analyzed and summarized in Table 25.

Out of the annual total SS discharge of 2,748,769.1 ton/year, most of the load comes from the diffuse source (99.8%) mostly through direct runoff (98.1%). The discharged SS load is transported to the watershed outlet and 69.6% of the load is reduced by the attenuation process. The remaining SS load of 836,546.4 ton/year flows to the Yellow Sea.

Out of the annual total BOD discharge of 79,215.1 ton/year, only 13.2% of the load comes from the point source while 86.8% comes from the diffuse source through direct runoff (71.0%) and baseflow (15.8%). The discharged BOD load is transported to the watershed outlet and 29.1% of the load is reduced by the attenuation process. The remaining BOD load of 56,143.3 ton/year flows to the Yellow Sea.

Out of the annual total TN discharge of 109,372.2 ton/year, only 24.8% of the load comes from the point source while 75.2% comes from the diffuse source through direct runoff (47.3%) and baseflow (27.9%). The discharged TN load is transported to the watershed outlet and 24.5% of the load is reduced by the attenuation process. The remaining TN load of 82,543.8 ton/year flows to the Yellow Sea.

Out of the annual total TP discharge of 10,893.3 ton/year, only 7.3% of the load comes from the point source while 92.7% comes from the diffuse source mostly through direct runoff (89.1%). The discharged TP load is transported to the watershed outlet and 65.2% of the load is reduced by the attenuation process. The remaining TP load of 3,788.3 ton/year flows to the Yellow Sea.

Table 25. Sources of pollution loads to the Yellow Sea from the Han River Watershed in 2016

Sources	SS		BOD		TN		TP	
	ton/year	%	ton/year	%	ton/year	%	ton/year	%
Point source	6860.7	0.2	10,481.7	13.2	27,120.8	24.8	792.8	7.3
Diffuse source	2,741,908.4	99.8	68,733.4	86.8	82,251.4	75.2	10,100.5	92.7
Direct runoff	(2,695,833.4)	(98.1)	(56,238.5)	(71.0)	(51,761.2)	(47.3)	(9,711.3)	(89.1)
Baseflow	(46,075.0)	(1.7)	(12,494.9)	(15.8)	(30,490.3)	(27.9)	(389.2)	(3.6)
Total discharge	2,748,769.1	100.0	79,215.1	100.0	109,372.2	100.0	10,893.3	100.0
Reduction by attenuation	1,912,222.7	69.6	23,071.8	29.1	26,828.4	24.5	7,105.0	65.2
Loads to the Yellow Sea	836,546.4	30.4	56,143.3	70.9	82,543.8	75.5	3,788.3	34.8

4 CONCLUSIONS AND SUGGESTIONS

4.1 Conclusions

To effectively decrease the pollution loads to the Yellow Sea, it is critical to understand how much pollution loads come from where and when. In RO Korea, there are four major river systems that flow to the Yellow Sea: the Han River, the Geum River, the Mankyoung-Dongjin River, and the Youngsan River. The pollution loads from each of these river systems need to be evaluated one by one. This study aims: (1) to set up a watershed model for the Han River Watershed; (2) to estimate the spatio-temporal distributions of pollution loads from the Han River Watershed to the Yellow Sea.

The Han River Watershed covers an area of 34,401.9 km^2 that accounts for 34.3% of the RO Korean territory. As a part of the river networks run across the RO Korea-DPR Korea border, the watershed lies in between the two countries: about four-fifths of the watershed area (27,919.8 km^2, 81.2%) lies in RO Korea, and the rest one-fifth of the watershed area (6,482.1 km^2, 18.8%) lies in DPR Korea.

Land-based pollution sources can be classified into two groups: point sources and diffuse sources. Point sources are any single identifiable sources of pollution such as pipes or drains. Factories and wastewater treatment plants are common point sources. Diffuse sources, on the other hand, occur over a wide area and are not easily attributed to a single source. They are often associated with particular land uses, as opposed to individual point source discharges.

The Han River Watershed encompasses both metropolitan cities such as Seoul, Incheon and other small to medium cities. The population in the Han River Watershed is about 20 million. Due to its dense population and intensive industrial/agricultural activities, the watershed has a great potential to discharge a large amount of pollution loads from both point sources and diffuse sources. The number of industrial operations in agri-industrial complexes in Seoul, Gyeonggi-do and Incheon within the Han River Watershed increased from 27,432 in 2007 to 46,864 in 2015. Industrial activities, among others, are more likely to discharge highly-concentrated pollutants. The growing number of industrial operations can result in increasing pollution loads from point sources. Attention should also be given to the fact that transportation of goods and people, closely related to industrial activities, can generate more potential for diffuse source pollution. The urban area increased by 397% from 323.2 km^2 in 1975 to 1,608.4 km^2 in 2010. The expansion of urban areas has led to the increase of impervious areas such as buildings and roads with concrete or asphalt surfaces. This would have caused a steep increase in accumulation and wash-off of urban diffuse source pollutants within the Han River Watershed. The agricultural area, on the other hand, shrunk by 29% from 5,358.9 km^2 in 1975 to 3,780.2 km^2 in 2010. However, a decrease in agricultural area doesn't necessarily mean a

decrease in agricultural diffuse pollution loads because the fertilizer application rate has increased and the use of plowing machines has increased the soil loss potentials, compared to the past.

Watershed models are widely used to evaluate pollution loads from various watersheds. As most environmental issues of a coast are closely associated with the characteristics of the watershed draining to the coast, certain features of watershed models such as mass balance analysis and scenario analysis are very useful to improve our scientific understandings of certain coastal processes and to derive reasonable alternatives.

Currently a wide range of various watershed models are being used to improve our understandings of the hydrologic and the hydrochemical processes within watersheds and to evaluate pollution loads discharged from watersheds, at the regional or global scale. Such watershed models include: IMAGE-GNM (Integrated Model to Assess the Global Environment-Global Nutrient Model), Global News-2 (Nutrient Export from WaterSheds version 2), SPARROW (SPAtially Referenced Regressions on Watersheds), RVERSTRAHLER, SWAT (Soil and Water Assessment Tool), STREAM (Spatio-Temporal River-basin Ecohydrology Analysis Model) and AGNPS (AGricultural Non-Point Source pollution).

Depending on the application purposes, watershed models can be very different from one another in terms of process representations, spatial scale, and temporal scale: some models simulate processes in detail using physically-based approaches while others use simple conceptual or empirical approaches; some models can be applied only at the watershed scale while others can be applied at the global scale; some models can be applied only for a short period of time while others can be applied for a very long period of time. Thus it is very important to select a right watershed model appropriate for the application purposes.

Taking into account the study scope, the limitations in data availability and the potential for extensions, the selection criteria for the watershed model for this study is set as the following:

- The model has appropriate structures to estimate pollution loads from both point and diffuse sources;
- The model is suitable to be applied to a very large watershed for a long period of time;
- The model can represent spatio-temporal distributions of pollution loads;
- The model's data requirements are low;
- The model's source codes are accessible for future extensions.

Based on the above criteria, REDPOLL (Regional Estimation of Diffuse POLlution Loads) was selected as the watershed model for this study. REDPOLL represents a watershed using a network of square grid cells. The model simulates hydrological processes using the SCS-CN methodology, and

estimates pollution loads on a daily basis using the event mean concentrations (EMCs) observed for different types of land uses. REDPOLL can represent spatio-temporal distributions of pollution loads discharged from diffuse sources within a large watershed such as the Han River Watershed, for a period of several years or more. As an intermediate-level model, REDPOLL does not require a heavy input data set and it can be set up and run with a relative ease. Moreover, research institutes have its source code, which suggests that it is likely to be expanded in the future. The source code of REDPOLL can be fully accessed by Korean government bodies for future extensions, if required.

The REDPOLL was set up for the Han River Watershed using grid cells of 100 m by 100 m and daily time steps for the year 2016. The precipitation and the temperature data observed at 18 monitoring stations in and around the Han River Watershed were collected and compiled for the model. The observed flow rates and water qualities of the discharges from main sewage treatment plants, the water abstractions from major dams within the watershed were collected and fed into the model. For estimating discharges from major dams, regression equations using the past observations of inflows, stages, and upstream precipitation are derived and incorporated into the model. Spatial distributions of topographic characteristics, land cover and soil texture were analyzed using the national data sets and compiled for the model.

The watershed model was calibrated against the flow rates and the water quality observed at the 48 sub-watershed outlets. The evaluated PBIAS (Percent BIAS, %) values of the calibrated model for flow rate, SS, BOD, TN and TP are 28.5%, 66.8%, 30.5%, 21.0%, and 53.2%, respectively. Given that the monitoring data were discontinuous, observed only on every 8 days, the calibration results are considered to be very good. It is particularly encouraging that the model calibration results of flow rates show very satisfactory (PBIAS = 16.0%, $R^2 = 0.68$) for 5 sub-watersheds where flow rates were observed continuously.

Flows and pollution loads to the Yellow Sea from the Han River Watershed were evaluated for the year 2016 based on the simulation results of REDPOLL. A water balance analysis of the Han River Watershed for the year 2016 show that out of the total annual precipitation of 1,100.6 mm/year (100%), evapotranspiration comprises 456.4 mm/year (41.5%), direct runoff and baseflow from the watershed comprise 629.2 mm/year (57.2%), and outflow to the Yellow Sea comprises 608.7 mm/year (56.2%).

For the year 2016, the annual total river flow from the Han River Watershed to the Yellow Sea is 21,286 x 10^6 m^3/year and the pollution loads are SS 836.5 x 10^3 ton/year, BOD 56.1 x 10^3 ton/year, TN 82.5 x 10^3 ton/year and TP 3.8 x 10^3 ton/year. River flows and pollution loads have a wide range of daily and monthly variation. As affected by the monsoon weather system, the monthly volume of river flows in July reaches 7,484 x 10^6 m^3/month accounting for 35.2% of the annual

discharge. Likewise, the monthly pollution loads in July comprise more than a quarter of the annual loads: SS 49.4%, BOD 40.0%, TN 30.9% and TP 41.6%.

In the Han River Watershed, the majority of pollution loads come from the diffuse source: SS 99.8%, BOD 86.8%, TN 75.2%, and TP 92.7%.

4.2 Policy Suggestions

4.2.1 Common research framework

In the context of the YSLME project, it is critical to estimate land-based pollution loads to the Yellow Sea from major river watersheds in RO Korea, DPR Korea, and PR China. For better understandings and development of effective national and international policies, it is of utmost importance to develop a common research framework for data sharing and common modeling platform among the three countries.

1) Data sharing

For common understandings of the environmental status of the watersheds draining to the Yellow Sea, it is essential to share environmental data among research scientists participating in the YSLME project. The list of data to be shared between research scientists should include:

- Boundaries of river basins and watersheds
- Topography
- Soils
- Geological formations
- Land covers/uses
- Population
- Livestock
- Significant point sources
- Use of inorganic and organic fertilizers
- Hydraulic structures
- Water abstractions

- Weather (precipitation, temperature, relative humidity, atmospheric pressure, wind velocity, solar radiation)
- Dam stages and discharges
- River flow rates
- River water quality (SS, BOD/TOC, TN, TP)

2) Common modeling platform

This study estimated pollution loads to the Yellow Sea from the Han River Watershed, using a watershed model REDPOLL. In the YSLME project, research scientists need to evaluate and compare pollution loads from various watersheds that are different in many aspects. Thus it is critical to apply a common evaluation methodology (i.e. a common modeling platform) to each of the watersheds. Without a common modeling platform, it would be very difficult and often disagreeable to compare and interpret the evaluation results from different models.

An example of applying a common methodology is the European Harmonised Procedures for Quantification of Nutrient Losses from Diffuse Sources (EUROHARP). EUROHARP was developed to report water quality predictions at national and international levels. It is a research project to set a common methodology that can be applied and incorporated to facilitate diffuse pollution estimation in Europe. EUROHARP was launched in a situation where a unified assessment methodology was needed among European countries, especially to fulfill science-based reporting requirements specified in key European Commission directives (Nitrates Directive, Water Framework Directive, Urban Waste Water Directive, etc.) and the Convention for the Protection of the Marine Environment of the North-East Atlantic (the OSPAR Convention).

EUROHARP helped build a nutrient estimation system, which enabled the application of consistent methods and reporting forms for quantifying nutrients from diffuse sources in Europe. A total of 17 European Union (EU) member states and 22 research institutes participated in this project. Nine representative models were selected for nutrient estimation (Table 26). These selected models are applied to 17 catchments including three core ones (Table 27) in EU (Figure 41) (Silgram *et al*., 2008). Each model must be applied to the core catchments, and additionally applied to three other catchments (in consideration of diversity in location and weather condition). Thus, each model is applied to at least six catchments.

Table 26. Nine representative models selected in EUROHARP and countries that have implemented the model (Silgram *et al*., 2008)

Models	Countries
ANIMO (Analysis of Networks with Interactive Modeling)	Denmark, Czech Republic, Germany, Netherlands
REALTA (Irish Model)	Germany, Lithuania, France
MONERIS(Modeling Nutrient Emissions in RIver Systems)	Lithuania, Ireland, Greece
TRK (Swedish Model)	Germany ,Netherlands, Hungary, France
N-LES (Danish Model)	Finland, Luxemburg, Spain
SWAT (Soil and Water Assessment Tool)	Sweden, Austria, Spain
EveNFlow	Germany, Czech Republic, Greece, United Kingdom
NOPOLU(Agricultural nonpoint emissions module)	All EU member states
Source apportionment	All EU member states

Table 27. Three core EU catchments modeled in EUROHARP (Silgram *et al*., 2008)

Catchment	Total area (km^2)	Agricultural land (%)	Annual Precipitation (mm/year)	Crops
Vansjo-Hobol, Norway	690	16	810	Cereals
Yorkshire Ouse, England	3,318	91	923	Cereals, Grass
Enza, Italy	922	70	1,000	Alfalfa

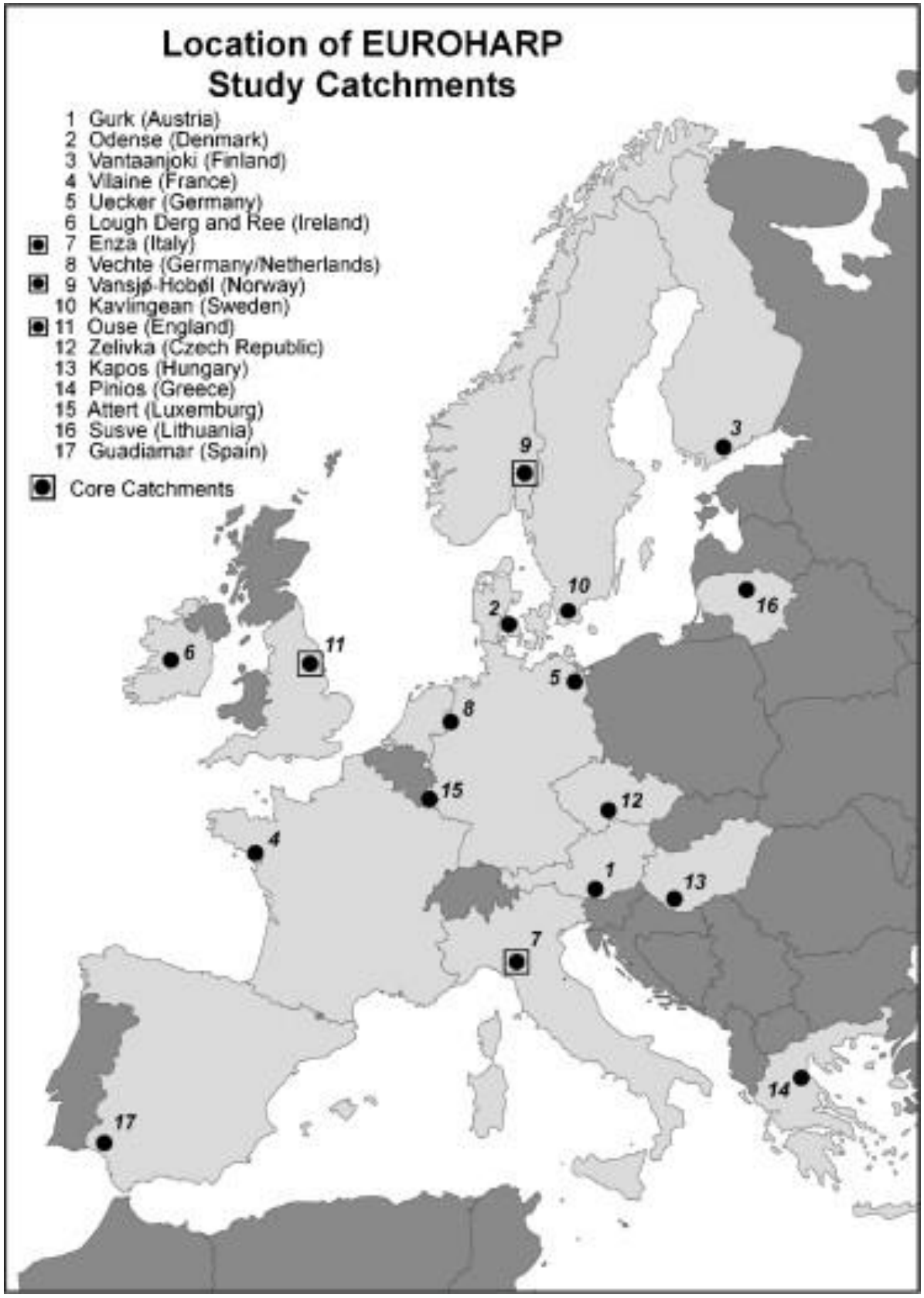

Figure 41. Location of the three "core" catchments used for more detailed analysis, and the location of the other catchments modeled in the EUROHARP project (Silgram *et al*., 2008)

EUROHARP is a pilot plan to build an integrated framework for diffuse pollution estimation models and reports that can be used among EU member states. There are no specific reports and cases of diffuse pollution estimation systems designated by any EU member state yet. As in the case of the EUROHARP Project, which attempts to unify estimation methods and reporting forms of different countries, RO Korea, DPR Korea and PR China need to agree on the methodologies for estimating pollution loads to the Yellow Sea. The criteria for selecting a common watershed model should include, but not limited to, the followings:

- Suitability to be applied to large watersheds
- Model structure to simulate temporal and spatial distribution of diffuse pollution loads
- Requirements for input data
- Flexibility for future expansion

For establishing a common modeling platform, scientists from three countries should discuss this issue as soon as possible. The common modeling platform may have more than one model and we suggest the REDPOLL model be used as one of the models in the common modeling platform.

4.2.2 Special concerns with PR China and DPR Korea

In this study, pollution loads to the Yellow Sea from the Han River Watershed were estimated. Although the Han River Watershed is relatively large and densely populated with high industrial operations in RO Korea, it accounts for only a small fraction of the total pollution loads to the Yellow Sea. To effectively manage the land-based pollution loads to the Yellow Sea, it is necessary to extend the geographical range of this study to other major river watersheds in RO Korea, DPR Korea, and PR China. Table 28 shows a list of major river watersheds draining to the Yellow Sea or the Bohai Bay. Note the watershed areas of the Chinese rivers are much larger than those of the Korean rivers.

○ PR China: the Bohai Bay

Although the Bohai Bay is connected to the Yellow Sea, it is excluded from the scope of the YSLME project. Considering the potential biophysicochemical processes between the Bohai Bay and the Yellow Sea, it is critical to include the Bohai Bay and its watersheds into the YSLME project. The Chinese river watersheds draining to the Bohai Bay and the Yellow Sea include: the Liao River, the Daling River, the Luan River, the Hai River, the Yellow River, the Huai River, and the Yangtze River.

Table 28. A summary of major river watersheds draining to the Yellow Sea and the Bohai Bay

Country	River	Watershed Area (km^2)	Outlet
RO Korea	Han	34,402	Yellow Sea
	Geum	9,912	
	Mankyoung-Dongjin	2,726	
	Youngsan	3,467	
DPR Korea	Aprok (Yalu)	62,295	
	Daedong	20, 344	
PR China	Yangtze	1,908,837	
	Huai	174,000	
	Yalu (Aprok)	62,295	
	Liao	192,645	Bohai Bay
	Daling	37,167	
	Luan	45,786	
	Hai	318,200	
	Yellow	843,108	

○ DPR Korea: Establishment of the partnership

Despite some of the DPR Korean rivers flow to the Yellow Sea, DPR Korea is not participating in the YSLME project for some reason. RO Korean authority needs to invite DPR Korean authority and should put more effort into establishing the partnership with DPR Korea in the context of this project. As the international politics are recently changing in favor of two Koreas, it may be a good time to make a move.

4.2.3 Inter-ministerial coordination

The Yellow Sea ecosystem is largely affected by land-based pollution loads. To successfully restore and manage the ecosystem, it is important to identify, evaluate and implement effective measures for land-based pollution sources. The Ministry of Environment is responsible for the land environment while the Ministry of Oceans and Fisheries is in charge of the marine environment. Although the land and the sea are connected to each other in nature, they are separately managed by the two ministries. It is therefore critical to establish a tight coordination system, such as liaison officers, between the two ministries to manage land-based pollution sources more efficiently and effectively.

REFERENCES

Alexander, R. B., Elliott, A. H., Shankar, U., & McBride, G. B. (2002). Estimating the sources and transport of nutrients in the Waikato River Basin, New Zealand. *Water resources research*, 38(12), 4-1.

Baker, M. (2002). Shorebirds of the Yellow Sea – importance, threat and conservation status. Wetland International, China. International Studies 12.

Barter, M.A. (2002). Shorebirds of the Yellow Sea: Importance, threats and conservation status. *Wetlands International Global Series 9, International Wader Studies, 12*: *104.*

Bashkin, V., Park, S., Choi, M., & Lee, C. (2002). Nitrogen Budgets for the Republic of Korea and the Yellow Sea Region. *Biogeochemistry*, 57/58, 387-403.

BOBLME. (2015). Results and achievements of the BOBLME Project.

Boughtons, W. C. (1989). A review of the USDA SCS curve number method. *Soil Research*, 27(3), 511-523.

Bricker, S. B., Longstaff, B., Dennison, W., Jones, A., Boicourt, K., Wicks, C., & Woerner, J. (2008). Effects of nutrient enrichment in the nation's estuaries: a decade of change. *Harmful Algae*, *8*(1), 21-32.

Chungbuk Research Institute. (2009). Improvement of Total-Maximum-Daily-Load Policy in Korea: Equity of Water Quality Standards and Management of Development Plans (published in Korean).

Cronshey, R. (1986). Urban hydrology for small watersheds. US Dept. of Agriculture. Soil Conservation Service, Engineering Division.

De'ath G, Fabricius KE, Sweatman H, Puotinen M.(2012) The 27– year decline of coral cover on the Great Barrier Reef and its causes. *Proc Natl Acad Sci USA*; 109:17995–17999.

Eagleson, P. S. (1978). Climate, soil, and vegetation: 5. A derived distribution of storm surface runoff. *Water Resources Research*, 14(5), 741-748.

Elliott, A. H., Alexander, R. B., Schwarz, G. E., Shankar, U., Sukias, J. P. S., and McBride, G. B. (2005). Estimation of nutrient sources and transport for New Zealand using the hybrid mechanistic-statistical model SPARROW. *Journal of Hydrology (New Zealand)*, *44*(1), 1.

Gilbert, P.M. (2014). Harmful Algal Blooms in Asia: an insidious and escalating water pollution phenomenon with effects on ecological and human health. *ASIA Network Exchange: A Journal for Asian Studies in the Liberal Arts*, 21(1), 52–68.

Great Barrier Reef Marine Park Authority. (2014). Great Barrier Reef: Outlook Report 2014. Australian Government, Townsville, Australia.

Hargreaves, G. H., & Samani, Z. A. (1985). Reference crop evapotranspiration from temperature. *Applied engineering in agriculture*, 1(2), 96-99.

Hassan, D. (2017). Protecting the Marine Environment from Land-Based Sources of Pollution: Towards Effective International Cooperation. Routledge, New York, USA.

Jeong, E.S., Cho, H.L., and Koo, B.K. (2018). Estimation of Pollution Loads to the Geum-River Estuary for Precipitation Conditions Using a Semi-distributed Watershed Model STREAM. *Journal of the Korean Society for Marine Environment and Energy,* 21(3), 216-227.

Keller, A. A., Chen, X., Fox, J., Fulda, M., Dorsey, R., Seapy, B., and Bray, E. (2014). Attenuation coefficients for water quality trading. *Environmental science & technology*, 48(12), 6788-6794.

Kremser, U., and Schnug, E. (2002). Impact of fertilizers on aquatic ecosystems and protection of water bodies from mineral nutrients. *Landbauforschung Volkenrode*, 52(2), 81-90.

Larcher, W. (2003). Physiological plant ecology: ecophysiology and stress physiology of functional groups. Springer Science & Business Media.

Moores, N., Kim, S-K., Park, S-B., and Sadayoshi, T. (2001). Yellow Sea Ecoregion: Reconnaissance Report on Identification of Important Wetland and Marine Areas for Biodiversity. *Volume 2: South Korea, WBK and WWF-Japan, Busan (published in Korean and English-language versions).*

Ministry of Environment. (2003). Green Korea 2003. Ministry of Environment (MOE), Republic of Korea.

Ministry of Environment (RO Korea), (2018). Environmental White Paper 2017.

Neitsch, S. L., Arnold, J. G., Kiniry, J. R., & Williams, J. R. (2011). Soil and water assessment tool theoretical documentation version 2009. Texas Water Resources Institute.

Novotny, V. (1986). A review of hydrologic and water quality models used for simulation of agricultural pollution. *Developments in environmental modeling*, 10, 9-35.

NRCS (Natural Resources Conservation Service). (1997). Ponds—Planning, design, construction.

Park, M. J., Shin, H. J., Park, J. Y., Kang, B. S., & Kim, S. J. (2009). Assessment of Climate and Vegetation Canopy Change Impacts on Water Resources using SWAT Model. *Journal of The Korean Society of Agricultural Engineers*, 51(5), 25-34.

Pedde, S., Kroeze, C., Mayorga, E., and Seitzinger, P. S. (2017). Modeling sources of nutrients in rivers draining into the Bay of Bengal - a scenario analysis. *Regional Environmental Change,* 17(8), 2495 - 2506.

Penman, H. L. (1947). Evaporation in nature. *Reports on progress in Physics, 11(1),* 366.

Ponce, V. M., & Hawkins, R. H. (1996). Runoff curve number: Has it reached maturity?. *Journal of hydrologic engineering,* 1(1), 11-19.

Rutherford, K. (2012). Modeling the effects of land use on nutrients entering the Tukituki River, Hawke's Bay. *A report prepared for Hawke's Bay Regional Council Ruataniwha Plains Water Storage Project*, 149.

SEPA (2004). Report on the state of the environment in PR China 2002. State Environmental Protection Administration (SEPA), Beijing, PR China.

She, J. (1999). Pollution in the Yellow Sea Large Marine Ecosystem: monitoring, research, and ecological effects. 419-426 in: Tang, Q and Sherman, K. (eds), Large Marine Ecosystems of the Pacific Rim: Assessment, Sustainability and Management. Blackwell Science, Malden, U.S. Sheibley, R. W., Konrad, C. P., & Black, R. W. (2015). *Nutrient attenuation in rivers and streams, Puget Sound Basin, Washingtons* (No. 2015-5074). US Geological Survey.

Shoemaker, L. (1997). Compendium of tools for watershed assessment and TMDL development.

Silgram, M., Anthony, G. S., Fawcett, L., and Stromqvist, J. (2008). Evaluating catchment-scale models for diffuse pollution policy support: some results from the EUROHARP project. *Environmental Science & Policy,* 11(2), 153 – 162.

Strokal, M., Yang, H., Zhang, Y., Kroeze, C., Li, L., Luan, S., Wang, H., Yang, S., and Zhang, Y. (2014). Increasing eutrophication in the coastal seas of PR China from 1970 to 2015. *Marine Pollution Bulletin,* 85(1), 123-140.

Strokal, M., Kroeze, C., Wang, M., Bai, Z., and Ma, L. (2016). The MARINA model (Model to Assess River Inputs of Nutrient to seAs): Model description and results for PR China. *Science of the Total Environment,* 562, 869-888.

Sutherland, R. C. (1980). An Overview of Stormwater Quality Modeling. In *Proceedings of the Seventh International Symposium on Urban Storm Runoff, University of Kentucky at Lexingtons*.

Teng, S.K., Yu, H., Tang, Y., Tonsg, L., Choi, C. I., Kang, D., Liu, H., Chun, Y., Juliano, R. O., Rautalahti-Miettinen, E. and Daler, D. (2005). Yellow Sea: GIWA Regional assessment 34. *University of Kalmar, Kalmar, Sweden.*

UN. (1994). United Nations Convention on the Law of the Sea - English. Available at: https://treaties.un.org/Pages/showDetails.aspx?objid=0800000280043ad5

UNDP/GEF. (2007). The Yellow Sea: Analysis of Environmental Status and Trends, Volume 2, Part I. National Reports – Republic of Korea.

UNDP/GEF. (2013). Reducing Environmental Stress in the Yellow Sea Large Marine Ecosystem. Special Meeting of the Project Steering Committee for the UNDP/GEF YSLME Project.

UNDESA. (2012). Review of implementation of Agenda 21: Detailed review of implementation of Agenda 21. *Stakeholder Forum for a Sustainable Future.*

USEPA. (2004). What is Nonpoint Source (NPS) Pollution? Questions and Answers. Available at: http://www.epa.gov/owow/nps/qa.html

USEPA. (2010). Chesapeake Bay Total Maximum Daily Load for Nitrogen, Phosphorus and Sediment. Available at: https://www.epa.gov/chesapeake-bay-tmdl/chesapeake-bay-tmdl-document

USEPA. (2017). An Overview of Rainfall-Runoff model Types. Office of Research and Development National Exposure Research Laboratory Athens, Georgia, U.S.

Wang, X., Williams, J. R., Gassman, P. W., Baffaut, C., Izaurralde, R. C., Jeong, J., & Kiniry, J. R. (2012). EPIC and APEX: Model use, calibration, and validation. *Transactions of the ASABE*, 55(4), 1447-1462.

Williams, J. R., and LaSeur, W. V. (1976). Water yield model using SCS curve numbers. *Journal of the hydraulics division*, 102: 1241-1253

Williams, J. R., Kannan, N., Wang, X., Santhi, C., and Arnold, J. G. (2011). Evolution of the SCS runoff curve number method and its application to continuous runoff simulation. *Journal of Hydrologic Engineering,* 17(11), 1221-1229.

WWF and KIOST. (2014). The ecosystems of the Yellow Sea: Summary report 2007 – 2014.

Zhao, W. L., Yang, S. Y., Wang, J., Xiao, J. M., Lu, X. X., Lin, J., Huang, P., & Cai, M. G. (2015). Load estimation and assessment of land-based pollution for Quanzhou Bay and their relevance to the Total Quantity Control of Pollutants Discharged into the Sea (TQCPS) Program in PR China. *Estuarine, Coastal and Shelf Science*, 166(B), 230-239.

Websites:

Ministry of Oceans and Fisheries (RO Korea). (2015).
http://www.mof.go.kr/article/view.do?articleKey=10299&boardKey=10&currentPageNo=1

Ministry of Environment (Government of Japan). (2018).
http://www.env.go.jp/en/water/wq/wemj/promot.html

USEPA. (2018). https://www.epa.gov/

WAMIS.(2018). http://www.wamis.go.kr/